Spring 2016

Quantifying the use of chloroform vapor exposure to improve the adhesion of Au Thin films onto PMMA

Kathleen T. Krist
James Madison University

Quantifying the Use of Chloroform Vapor Exposure to Improve the Adhesion of Au Thin Films onto PMMA

An Honors Program Project Presented to

the Faculty of the Undergraduate

College of Science and Mathematics

James Madison University

by Kathleen Taylor Krist

April 2016

Accepted by the faculty of the Department of Chemistry and Biochemistry, James Madison University, in partial fulfillment of the requirements for the Honors Program.

FACULTY COMMITTEE:

Project Advisor: Wm. Christopher Hughes, Ph.D.,
Professor, Physics and Astronomy

Reader: Barbara A. Reisner, Ph.D.,
Professor, Chemistry and Biochemistry

Reader: Brycelyn M. Boardman, Ph.D.,
Assistant Professor, Chemistry and Biochemistry

HONORS PROGRAM APPROVAL:

Bradley R. Newcomer, Ph.D.,
Director, Honors Program

PUBLIC PRESENTATION

This work is accepted for presentation, in part or in full, at the JMU Honors Symposium on April 15, 2016.

Table of Contents

List of Figures

Figures

Tables

Images

Acknowledgements

This work was supported by the National Science Foundation – Research in Undergraduate Institutions grant DMR#1305808. I would like to thank Dr. Chris Hughes with the JMU Department of Physics and Astronomy and Drs. Barbara A. Reisner and Brycelyn M. Boardman with the JMU Department of Chemistry and Biochemistry for serving on my committee. Finally, I would like to acknowledge Dr. Harry Hu for designing the force-measuring device, Mr. Skylar N. White for acquiring the AFM images presented in this work, and Ms. Yvonne M. Kinsella for assisting with PMMA sample preparation and metal deposition.

Abstract

The metallization of Au onto plastics is an important processing step in applications such as the aerospace and automotive industries, the field of microelectronics, and the fabrication of microfluidic devices. While its corrosion resistance and excellent electrical and thermal conductivity make Au a useful choice, its inertness results in poor adhesion to polymer surfaces. Previous studies have indicated that exposing commercially available poly(methyl methacrylate) (PMMA) sheets to chloroform vapor following Au deposition significantly improves adhesion. In this study, we utilized electron-beam evaporation and magnetron sputtering to deposit Au thin films onto 1.50 mm thick PMMA and exposed the samples to vapor released from chloroform heated on a hot plate set at 70 °C. The force required to remove both treated and untreated Au thin films was determined by placing samples on a polisher spinning at 150 rpm and utilizing UV-VIS spectroscopy to measure the absorbance of light through the films to quantify their removal as a function of applied polishing force. The pressure required to polish Au from PMMA exposed to chloroform ($CHCl_3$) after metal deposition was compared to the pressure required for pre-treated samples. Post-treated Au thin films were characterized during the polishing process using atomic force microscopy (AFM). AFM images demonstrated a progressive roughening of the surface corresponding to an increase in applied force. Additionally, these images support a model in which the chloroform treatment softens the PMMA surface, producing a softened layer that the polisher removes simultaneously with the Au thin film. The chloroform post-treatment procedure was then used to selectively pattern a series of PMMA samples.

Introduction

The deposition of metal thin films onto polymeric substrates (plastics) to incorporate electrodes and connecting wires is an important processing step in the fabrication of sensors and microelectronic elements. These components are essential in the assembly of aeronautical and automotive vehicles, the development of devices such as smart phones and personal computers, and the fabrication of microfluidic devices for studying microbiological systems.[1-4] Gold (Au) is an ideal metal for fabricating electrodes, interconnecting wires, and optical elements due to its high electrical and thermal conductivity,[1] high corrosion resistance, and excellent reflectivity, particularly of infrared light. Polymers are widely used due to their manufacturability, low cost, high strength-to-weight ratio, and biocompatibility.[1,5-7] Unfortunately, Au is an inert metal, and its adhesion onto polymeric surfaces is notoriously poor. The relatively strong cohesive forces holding the Au atoms together prevent chemical bonding between the adsorbed metal atoms and the polymer surface.[1-3]

Process engineers in the semiconductor industry have previously utilized a metal adhesion layer for improving the adhesion of Au onto silicon-based substrates. This adhesion layer is deposited directly onto the silicon surface prior to Au deposition and consists of a reactive metal such as chromium or titanium. The layer can adhere to the Au atoms and bond with the polar atoms at the silicon surface. Because the polymeric substrates of interest are mostly nonpolar, the use of an adhesion layer is of limited utility. Researchers have instead developed modifications for enhancing Au adhesion by polarizing the polymer surface. Methods such as chemical etching, ultraviolet irradiation, and plasma treatment typically involve adding polar bonds or increasing surface roughness. Most of the aforementioned techniques have resulted in limited success and pose the risk of otherwise modifying the polymer surface.[1,3]

1. Utilization of polar solvents for improving the adhesion of Au onto PMMA.

Previous studies conducted by the Hughes-Augustine Lab at James Madison University have focused on improving the adhesion of Au thin films onto sheets of poly(methylmethacryate) (PMMA), a commercially available plastic known as plexiglass or acrylic. In their initial discovery, Mo et al.[3] enhanced Au-PMMA adhesion by spin-casting organic solvents directly onto the polymer surface. Samples were spun-cast with hexanes, toluene, or chloroform, listed here in order of increasing polarity. Within 10 minutes of treatment, a thin layer of Cr followed by a Au thin film was magnetron sputter deposited onto each PMMA sample through a shadow mask containing circular features. The Cr adhesive layer was 10 Å thick, and an average thickness of 540 Å was measured for the Au film.

Au-PMMA adhesion was measured by performing a tape-pull test. A piece of clear tape was applied to each sample and abruptly ripped off in order to remove as much metal from the PMMA surface as possible. Pictures of the PMMA samples before and after the tape-pull test were obtained using a microscope and digital camera. The data were analyzed by comparing the number of black pixels before and after the tape-pull test, where each black pixel corresponded to an area of surface covered by Au atoms (Figure 1). Following the tape-pull test, only 20% of the area covered by Au remained coated on the untreated control sample. Treating the surface with O_2 plasma only improved adhesion to 26% Au remaining, and the spin-casting of hexanes actually decreased the adhesion percentage to 2%. The samples spun-cast with toluene improved the adhesion percentage to approximately 50%, and the samples spun-cast with $CHCl_3$ improved Au adhesion to nearly 90%. These results indicated that Au-polymer adhesion can be enhanced by spin-casting polar solvents onto the PMMA surface.

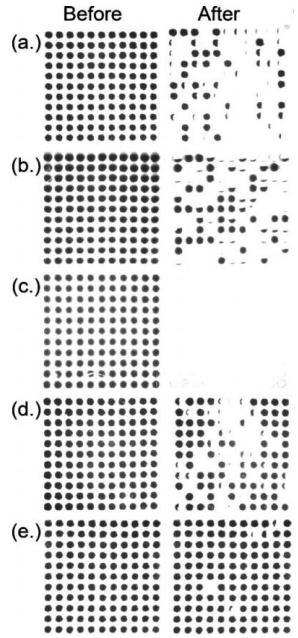

Figure 1. Optical micrographs depicting 11 X 11 Au dot arrays (~1.5 mm in diameter) on PMMA. The left column shows samples after Cr/Au deposition but before the tape-pull test. The right column depicts samples following the tape-pull test. a) control b) O_2-plasma-treated c) hexane-cast d) toluene-cast e) $CHCl_3$-cast. Taken from Mo et al.[3]

2. Elucidation of a mechanism explaining the effectiveness of $CHCl_3$ pre-treatment.

A single chloroform molecule consists of a central carbon atom bonded to three chlorine atoms and one hydrogen atom (Figure 2). The element chlorine belongs to a group of reactive nonmetals known as the halogens. Because the PMMA samples spun-cast with $CHCl_3$ yielded the best Au-PMMA adhesion results, Mo et al.[1] explored the use of two other halogenated solvents, bromoform ($CHBr_3$) and fluoroform (CHF_3). PMMA samples spun-cast with $CHCl_3$ or $CHBr_3$ or exposed to gas-phase CHF_3 were coated with 10 Å of Au or platinum (Pt) using electron-beam evaporation. While the $CHCl_3$ and $CHBr_3$ treatments increased the metal-PMMA adhesion for both Au and Pt thin films, the gaseous CHF_3 exposure showed no improvement over O_2 plasma-treated or untreated samples. Mo et al.[1] also found that exposing Au-plated PMMA to room temperature $CHCl_3$ vapor for 300 s improved Au-PMMA adhesion.

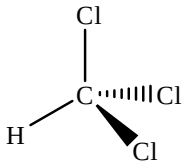

Figure 2. Chloroform ($CHCl_3$).

Mo et al.[1] developed an explanation for the efficacy of halogenated solvent pre-treatment using a variety of experimental techniques and computational modeling. PMMA is a chain of repeating ester groups, each of which consist of a carbon atom double-bonded to an oxygen atom and single-bonded to a second oxygen atom (Figure 3).

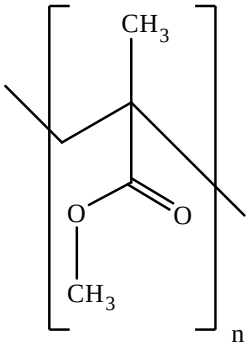

Figure 3. Structure of poly(methyl methacrylate) (PMMA).

Upon exposure to $CHCl_3$ or $CHBr_3$, residual solvent molecules remain on the PMMA surface long after most of the solvent evaporates. These molecules chemically activate the surface through the formation of a Lewis acid-base adduct between the single-bonded oxygen atom of the PMMA and the hydrogen atom of the solvent (Figure 4a). During metal deposition, a Au or Pt atom is introduced into the Lewis acid-base adduct and inserted into the C-Cl or C-Br bond (Figure 4b-c). The resulting bonding configuration consists of a metal atom situated between the single-bonded oxygen of the PMMA and the halogen atom of the solvent (Figure 4d). Chlorine and bromine are highly electronegative elements, meaning they tend to withdraw electrons from

other atoms in a chemical bond. When either halogen atom is bonded to a metal such as Au or Pt, the halogen withdraws electron density from the metal atom. This electron-deficient metal atom engages in an energetically stable interaction with the electron-rich single-bonded oxygen atom of the PMMA, and this stability accounts for the adherence of the metal onto the PMMA surface.

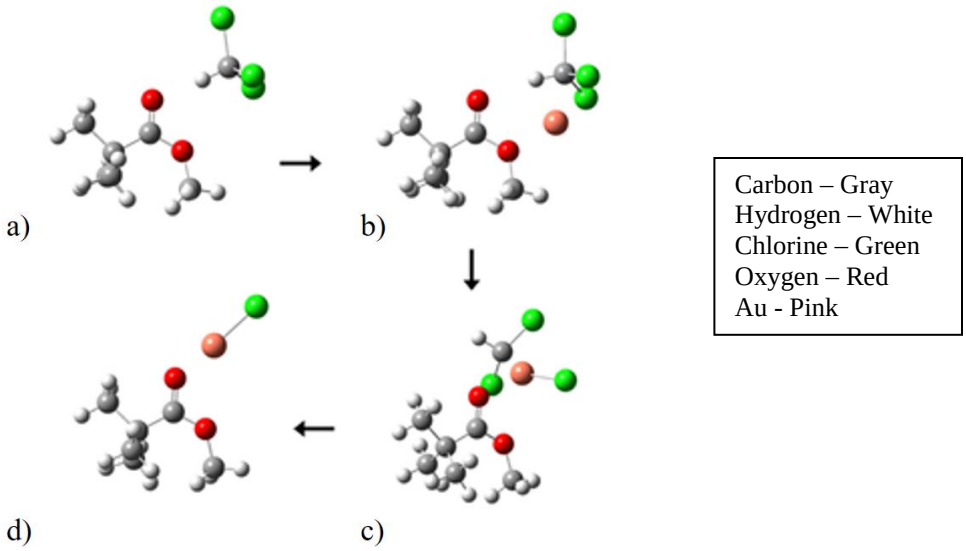

Figure 4. Model of Au-$CHCl_3$-PMMA interaction as determined by density functional theory. a) Formation of Lewis acid-base adduct between the $CHCl_3$ molecule and the single-bonded oxygen of PMMA, b) introduction of Au atom into the Lewis acid-base adduct, c) insertion of Au atom into C-Cl bond of $CHCl_3$ and d) O-M-Cl adsorbate remaining after solvent evaporation. Taken from Mo et al.[1]

This mechanism also explains the failure of CHF_3 gas-phase exposure to promote the adherence of Au and Pt onto PMMA. The energies of the bond strengths for Au-Cl and Au-Br are lower than the energies for C-Cl and C-Br, respectively. The fact that the energies of the reactants are higher than those of the products promotes the formation of a Au-halogen bond. Because the energy of the bond strength for Au-F is higher than the energy for C-F, the metal atom will not insert itself into the C-F bond.

The importance of the Lewis acid-base adduct in the aforementioned mechanism prompted Mo et al.[1] to compare the viability of pre-treatments using complexing and non-complexing solvents. For a complexing solvent, the Lewis acid-base interactions between the polymer of interest and solvent are limited, and polymer chains can aggregate to form a complex in solution. In the case of PMMA, the dipole moments of the polar ester groups account for the interactions between chains. A non-complexing solvent forms a strong Lewis acid-base adduct with a polymer and prevents interactions between the polymer chains by shielding the dipole moment. The three complexing solvents tested were hexanes, tetrahydrofuran, and carbon tetrachloride, and the two non-complexing solvents were $CHCl_3$ and dichloromethane. As expected, exposure to the two non-complexing solvents improved Au-polymer adhesion significantly in comparison to the complexing solvents.

3. Introduction of post-chloroform vapor exposure. Most recently, Mo et al. have demonstrated that using $CHCl_3$ post-treatment in place of pre-treatment also significantly improves the adhesion of the Au onto the plastic. They have developed a new vapor exposure method in which 60 Å of Au are deposited onto the PMMA using electron-beam evaporation and the sample is then exposed to $CHCl_3$ vapor heated at 70 ºC for 5 seconds. Roughly half of the Au-plated surface is concealed by a sheet of poly(dimethylsiloxane) (PDMS) plastic during exposure so that the resulting surface contains both treated and untreated portions of Au. The PDMS is peeled off the PMMA surface following vapor exposure, and the metal thin film is removed by polishing the sample. Because the untreated Au disappears from the PMMA almost immediately and often completely before removal of the treated Au is readily apparent, this test provides excellent qualitative evidence for the efficacy of $CHCl_3$ post-treatment. Quantitative data are still needed to demonstrate the usefulness of $CHCl_3$ vapor exposure.

This study reports the development and implementation of a method for obtaining quantitative data that measures the effectiveness of post-Au deposition $CHCl_3$ vapor exposure in improving the physical adhesion of Au thin films onto PMMA. Both quantitative and qualitative data are presented to confirm the viability of $CHCl_3$ post-treatment as a technique for improving the wear resistance of Au deposited onto PMMA. A comparison between implementing the $CHCl_3$ vapor exposure prior to Au deposition versus post-deposition exposure is also reported. Finally, the ability to selectively pattern materials using $CHCl_3$ vapor exposure will be discussed.

Experimental Section

Substrate Preparation. PMMA sheets (1.50-mm thick, McMaster-Carr) were cut into 2.54 cm x 2.54 cm squares using a VLS 3.50 laser cutter. Samples were cleaned by ultrasonication in 2-propanol for 10 minutes at room temperature and blown dry with N_2 gas. Each sample intended for use as a blank during data acquisition was covered by a 2.54 cm x 2.54 cm sheet of poly(dimethylsiloxane) (PDMS) film (600-µm thick, Stockwell Elastomerics). The 2-propanol (Certified ACS Plus) was used as received from Fisher Scientific.

Au Deposition. PMMA samples were metallized with Au either by electron-beam (e-beam) evaporation or by magnetron sputtering. Both methods are classified as physical vapor deposition (PVD), a family of processes in which gas phase atoms are deposited onto a solid substrate under vacuum.[8] In e-beam evaporation, substrates are placed in a sample holder mounted to the ceiling of a vacuum chamber (Figure 5). A motor rotates the sample holder and ensures homogeneous deposition among the samples. The chamber floor houses a tungsten filament that emits a focused beam of high energy electrons (e-beam) when connected to a power supply. This e-beam is swept across a metal-containing crucible located directly beneath the sample holder. The energy transferred from the beam to the crucible vaporizes the metal atoms, which translate upwards and precipitate onto each substrate to produce a solid thin film.

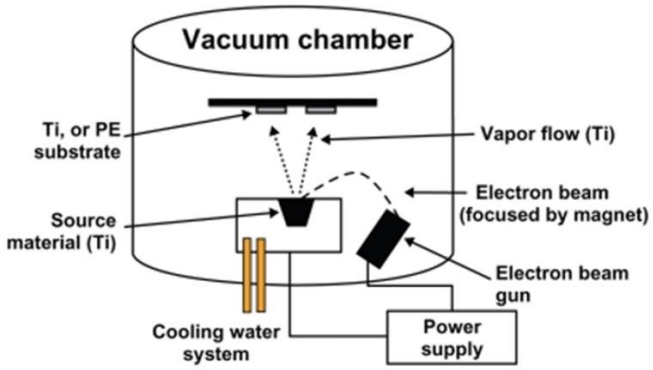

Figure 5. Electron-beam evaporation. Taken from Raimondo et al.[9]

Prior to deposition, air is evacuated from the chamber until the pressure reaches ~10^{-5} mbar. This low pressure environment allows the Au atoms to travel to the sample surface without colliding with other atoms and inhibits water vapor, oxygen gas, and other air-borne particulates from contaminating the metal thin film. Due to the high-energy nature of the electron beam, e-beam evaporation is ideal for depositing materials with high melting points such as Au.[8,10,11]

Magnetron sputtering utilizes plasma instead of an e-beam to deposit metal thin films onto a substrate. A rotating sample holder is mounted to the ceiling of a vacuum chamber, and air is pumped out of the chamber until the pressure falls below 10^{-4} Torr. The plasma is generated by exciting argon gas to form positively charged ions. A direct current power supply generates a positive voltage that creates the plasma and accelerates the argon ions through an electric field towards a negatively charged electrode. This "target" is located at the bottom of the chamber and contains a solid metal plate of high purity (Figure 6). The positive ions strike the target with enough force to eject the metal atoms, which condense onto the bottom of each substrate to form a thin film. As with e-beam deposition, the low pressure reduces contamination by background gases and minimizes collision-induced energy losses that inhibit the metal atoms from reaching the substrate.[8,12]

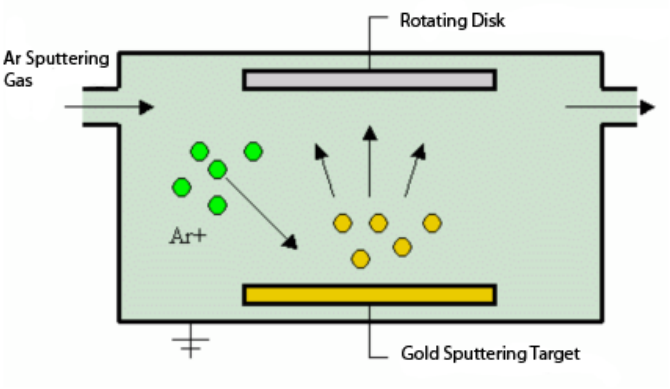

Figure 6. Magnetron sputtering. Taken from Mo et al.[13]

60 Å of Au were deposited onto PMMA at a rate of 1 Å/s using an mBRAUN e-beam evaporator. Au thin film thickness was monitored by a quartz crystal microbalance (QCM). 140.7 ± 34.8 Å of Au were deposited onto PMMA for 90 s at 75 W using an Edwards AUTO 500 magnetron sputtering system. Au film thickness was measured using a KLA Tencor P-7 Stylus Profiler. For both PVD processes, samples covered with PDMS were placed in the chamber during deposition but were not metallized.

$CHCl_3$ Vapor Exposure. A $CHCl_3$ vapor bath was prepared by pouring $CHCl_3$ (~50 mL) into a glass petri dish (9-cm diameter) covered with a glass lid (9.5-cm diameter) and heating the liquid at 70 °C for 10 minutes. During the heating period, Au-plated and blank PMMA samples were mounted to the inside of a glass petri dish lid using a PDMS film. The samples were then exposed to the $CHCl_3$ vapor by covering the dish for 5 s. For pre-treatment studies, PMMA samples were exposed to $CHCl_3$ vapor within 10 minutes prior to Au deposition. For post-treatment studies, PMMA samples were exposed to the $CHCl_3$ vapor immediately following metallization. The $CHCl_3$ (Certified ACS) was used as received from Fisher Scientific.

Au Thin Film Removal. To obtain quantitative data demonstrating the efficacy of $CHCl_3$ vapor exposure, the amount of force required to remove the Au film from the surface of a $CHCl_3$-treated sample was compared to the force required to remove Au from an untreated substrate. The Au was polished off each sample using an Allied High Tech Products polisher spinning at 150 revolutions per minute. The adhesive back polishing cloth (8 in.) was used as obtained from Allied High Tech Products.

The quantity of force applied onto each sample was controlled using a specially designed force-measuring device. The first generation device was used to obtain quantitative data for Au-plated PMMA samples prepared by e-beam evaporation. This apparatus consisted of a hollow

brass cylinder inserted into an aluminum metal bar. The cylinder contained a stainless steel spring attached to a steel screw and a sample mounting disk (Figure 7).

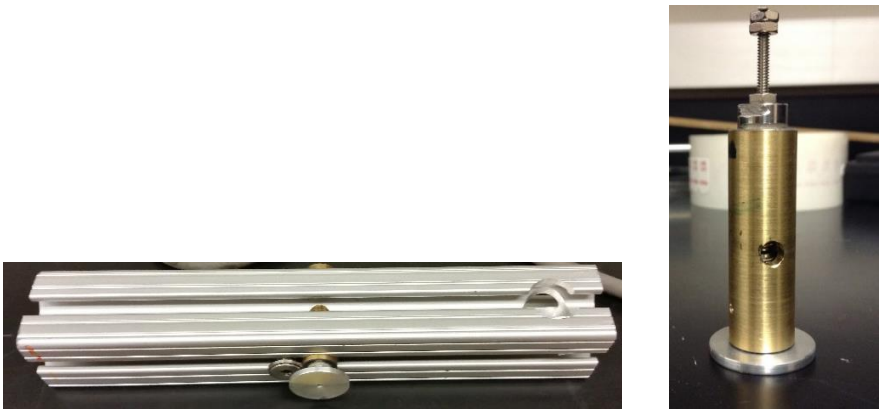

Figure 7. First generation force-measuring device (left) and brass cylinder component (right).

A PMMA sample was taped to the bottom of the disk using Scotch double-sided adhesive, and the force-measuring device was situated so that the Au-plated PMMA surface was directly above the polishing cloth (Figure 8). The device was zeroed by running the polisher and turning the screw until a slight scratching sound was heard. This sound indicated when the sample first came in contact with the polishing pad.

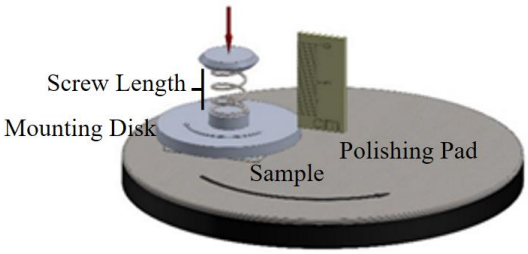

Figure 8. Schematic depicting the polishing process using the first generation force-measuring device. The gray disk represents the polishing pad spinning counterclockwise, and the PMMA sample is mounted onto the bottom of the

stationary light blue disk. Compressing the spring increases the quantity of force applied onto the PMMA sample. Reproduced with permission from Harry Hu.

Turning the screw clockwise compressed the spring, which in turn exerted a force on the mounted sample. This compression corresponded to a linear increase in force according to Hooke's Law. Force increments were defined as a change in screw length (Figure 8) equal to approximately 0.10 mm. For each increment of force applied, the sample was polished for 5 s.

Data for Au-plated PMMA samples prepared by magnetron sputtering were obtained using a second generation force-measuring device that incorporated a load cell into the design (Figure 9). A load cell is a sensor that generates a measurable electrical output, such as a voltage or current, in response to a mechanical force.[14] The output can be converted into a digital reading and is directly proportional to the applied force.

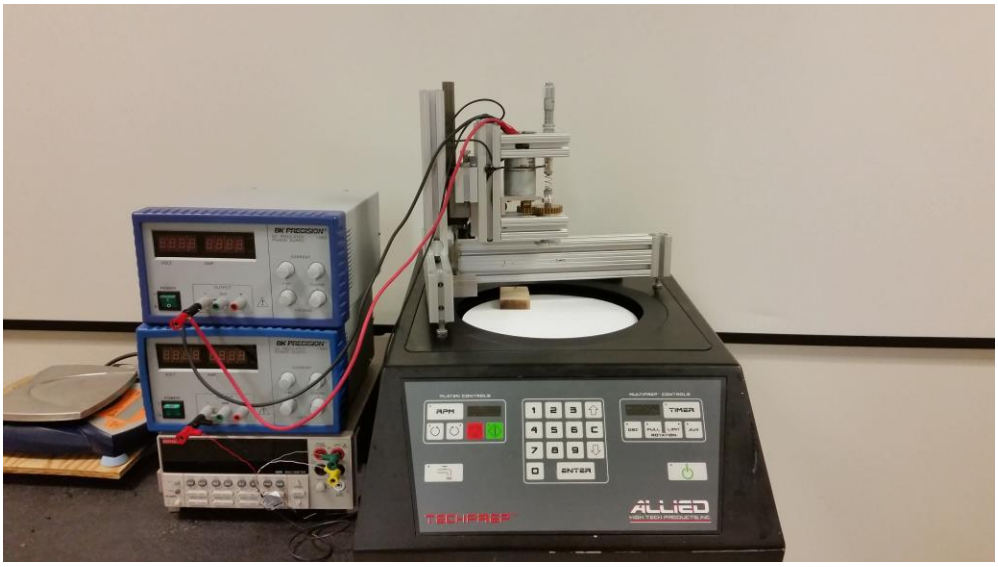

Figure 9. Complete Au removal setup using the second generation force-measuring device.

The load cell (Futek LSB200) was powered with 10.5-12 V from a BK Precision DC regulated power supply and sandwiched between a caliber and a stainless steel spring. Turning the caliber

clockwise compressed the spring, which in turn exerted a compressive force on the mounted PMMA sample (Figure 10). The load cell converted this force into a voltage that was digitally monitored using a Keithly 2000 multimeter. An increase in the voltage reading corresponded to an increase in the force applied onto the PMMA sample. A Cytron Technologies DC motor powered with 5 V from a BK precision DC regulated power supply was connected to the sample mounting disk. Rotating the sample clockwise while the polishing pad was spinning counterclockwise ensured that the Au-plated PMMA surface was polished evenly (Figure 10). The device was zeroed by running the polisher and turning the caliper until a slight scratching sound was heard. This sound indicated when the sample first came in contact with the polishing pad. An increment of force was designated as an approximately 0.10 mV reading from the load cell. For every force increment applied, the sample was polished for 20 s.

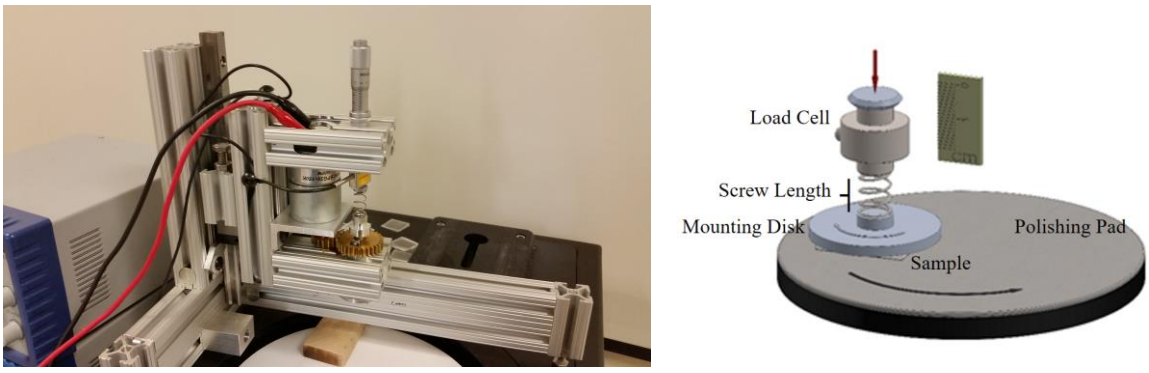

Figure 10. Second generation force-measuring device (left). Schematic depicting the polishing process (right). While the polishing pad (light gray disk) is spinning counterclockwise, a motor rotates the mounted sample (light blue disk) clockwise to ensure the Au-plated surface is evenly polished. Compressing the load cell converts the mechanical force into a digital voltage reading that is directly proportional to the applied force. Reproduced with permission from Harry Hu.

Force-measuring Device Calibration. The force-measuring devices were calibrated using a Scout Pro 1000 g balance. The first generation device was clamped onto a milling machine table, and the sample mounting disk was situated directly above the balance. To zero the device, the screw was turned clockwise until the mounting disk barely touched the scale and the digital reading was 0.0 g. For every decrease in screw length of ~0.10 mm, the mass was recorded. The scale was placed on the polisher beneath the sample mounting disk (Figure 11). To zero the device, the caliper was turned clockwise until a scale reading of 0.0 g was obtained with the mounting disk just barely touching the scale surface. For every caliper rotation equivalent to 0.20 mm, the mass reading on the scale and the corresponding voltage were recorded.

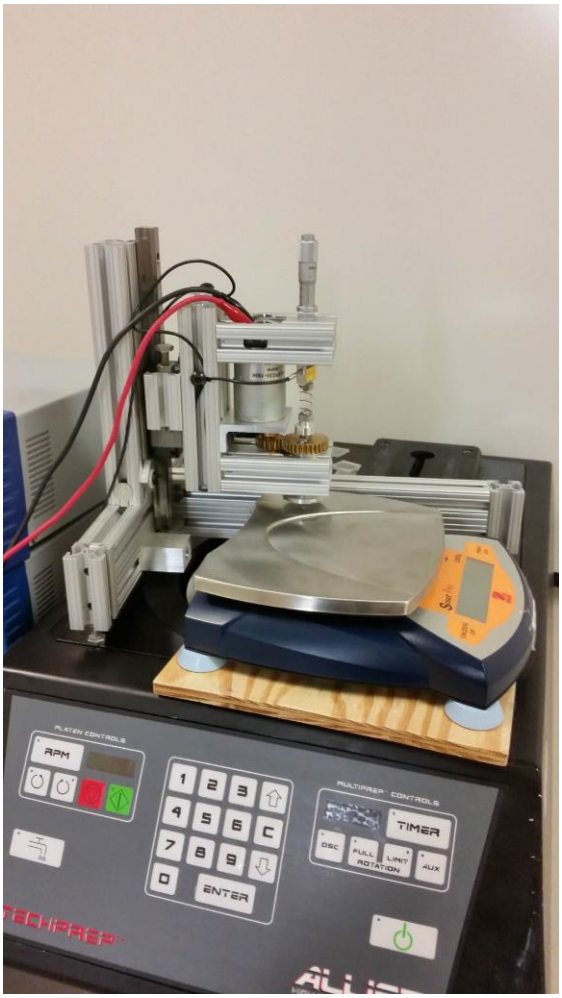

Figure 11. Calibration setup for second generation force-measuring device.

UV-VIS Spectra Acquisition. For every force increment used to polish a Au-coated PMMA sample, quantitative data were obtained using ultraviolet-visible (UV-VIS) spectroscopy. A typical spectroscopic experiment utilizes the diffraction of white light into multiple wavelengths to analyze the contents of a specific compound (analyte). A beam of light containing visible wavelengths from a tungsten lamp source and ultraviolet light from a deuterium lamp is directed towards a quartz container (cuvette) containing the analyte solution (Figure 12).

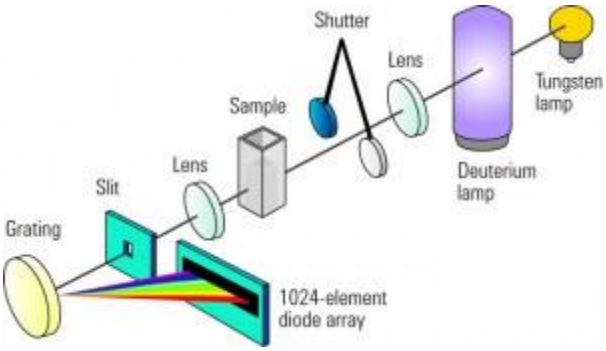

Figure 12. UV-VIS Spectroscopy. Taken from nanoComposix.[15]

The light is either absorbed by the particles in solution, scattered, or transmitted through the solution. The transmitted light is separated into each of its component wavelengths using a diffraction grating, and the intensity (I) of each individual wavelength is detected electronically. This measurement is compared to the intensity of a reference beam (I_o) that passes through a cuvette containing only solvent (the blank). Because the analyte solution contains more light-absorbing particles than the pure solvent, the detected light from the sample is always less intense. The ratio I/I_o is known as transmittance, and the % transmittance (%T) is calculated by the following equation:

$$(1) \quad \%T = \left(\frac{I}{Io}\right) * 100$$

The spectrometer scans all wavelengths from 200-900 nm and plots the transmittance as a function of wavelength to generate a spectrum. The absorbance (A) measures the quantity of light trapped by the particles in solution and is calculated by the following equation:

$$(2)\quad A = \log\left(\frac{1}{T}\right)$$

A positive linear correlation relates the absorbance of light by a solution to the concentration of that solution (c), according to the Beer's Law equation:

$$(3)\quad A = abc$$

The molar absorptivity (a) of light is an inherent property of each solution, and the path length (b) is the distance the light must travel to pass through the sample. By obtaining spectra for solutions containing different concentrations of analyte, a linear calibration curve plotting the absorbance at a specific wavelength versus concentration can be generated. The wavelength of maximum absorbance is chosen to maximize linearity and sensitivity. This plot can be used to determine the concentration of analyte in an unknown sample through interpolation.[16,17]

The theory behind UV-VIS spectroscopy can be applied to the removal of Au from PMMA. Polishing reduces the number of Au particles on the plastic surface and progressively allows more light to pass through the sample and reach the detector. The absorbance of light by the PMMA decreases as force applied onto the sample increases and reaches zero once all Au has been removed relative to a PMMA-only blank.

Absorbance spectra were acquired using an Agilent Technologies UV-VIS Spectrophotometer. The path length was set at the thickness of the PMMA samples (0.15 cm). Initial spectra were obtained for each sample prior to gold removal, and further spectra were taken for every increment of force applied onto the PMMA. Blanks required for calibrating the

spectrophotometer were prepared by subjecting clear PMMA squares to the same temperature, pressure, and $CHCl_3$ exposure conditions as the corresponding Au-plated samples. To observe the morphology of the samples during various stages of the Au removal process, atomic force microscopy (AFM) images were obtained using a Nanoscope Dimension 3100.

Selective Patterning. Selective patterning is a microfabrication technique that can be used to plate metal onto specific areas of a given surface. Patterned arrays were designed using CorelDraw and printed onto square PDMS masks (2.54 cm x 2.54 cm) using a VLS 3.50 laser cutter. Approximately 140.7 ± 34.8 Å of Au were deposited onto substrates using magnetron sputtering. After covering each sample with a PDMS mask, the chloroform vapor exposure described in *$CHCl_3$ Vapor Exposure* was implemented. The masks were then removed, and each PMMA surface was wiped using a KimWipe.

Results and Discussion

Quantifying the efficacy of $CHCl_3$ post-treatment using the first generation force-measuring device. The calibration curve produced for the first generation force-measuring device is shown in Figure 13. The equation for the line of best fit was used to determine the pressure applied to every PMMA sample as controlled by the adjustment of a screw. The pressure was calculated from the force equivalent to a mass on a balance. The line of best fit is given by Equation 4:

$$y = 43.885x - 0.0627 \quad (4)$$

where x is the difference between the initial screw length and the caliper reading for a given force increment, and y is the mass corresponding to that increment.

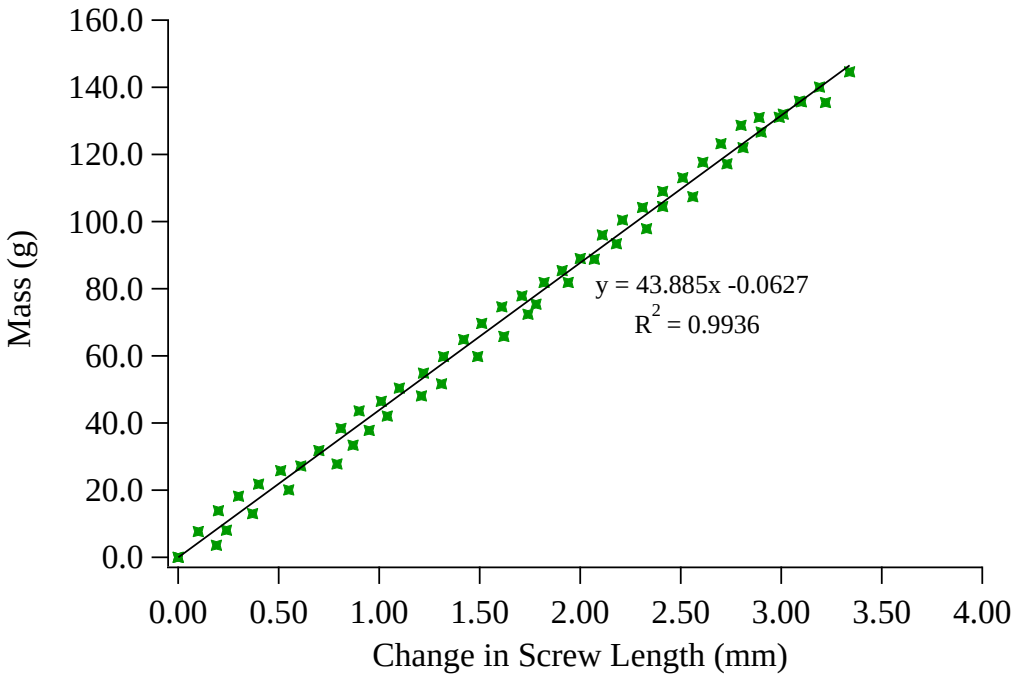

Figure 13. Calibration of the first generation force-measuring device. This plot combines the data from two separately obtained mass-distance curves (Supporting Information, Figure S1). A value of 0.0 mm along the x-axis corresponds to the initial screw length and a 0.0 g reading when the force-measuring device is just touching the scale

surface. The change in distance for a given force increment is defined as the difference between the initial screw length and the current caliper reading.

The y-intercept needed to correlate a mass of 0.0 g to a screw extension of 0.0 mm was determined by substituting the initial screw length for x and setting y = 0. The initial screw length varied among PMMA samples. The modified y-intercept was then substituted for the original intercept in Equation 4, and the mass corresponding to each 5 s polishing process could be calculated. To obtain the force in Newtons (N), each mass was multiplied by the gravitational acceleration constant according to Equation 5:

$$(5) \quad F = mg$$

where F is force (N), m is mass (kg), and g is the gravitation acceleration constant.
The pressure in pascals was then calculated for each force increment using Equation 6:

$$(6) \quad P = F/A$$

where P is pressure and A is the area of a PMMA square (m^2).

The absorbance spectra obtained for each polishing process for an untreated sample are shown in Figure 14. The spectral patterns obtained while polishing a sample exposed to $CHCl_3$ vapor exposure are displayed in Figure 15. The absorbance values observed at 850 nm for both samples were plotted as a function of applied pressure to generate two S-shaped curves (Figure 16). A wavelength of 850 nm was chosen due to its proximity to the wavelength of maximum absorbance. While only the data for a single treated and single untreated Au-coated PMMA sample are presented here, additional pressure curves can be found in the Supporting Information (Figures S2 and S3).

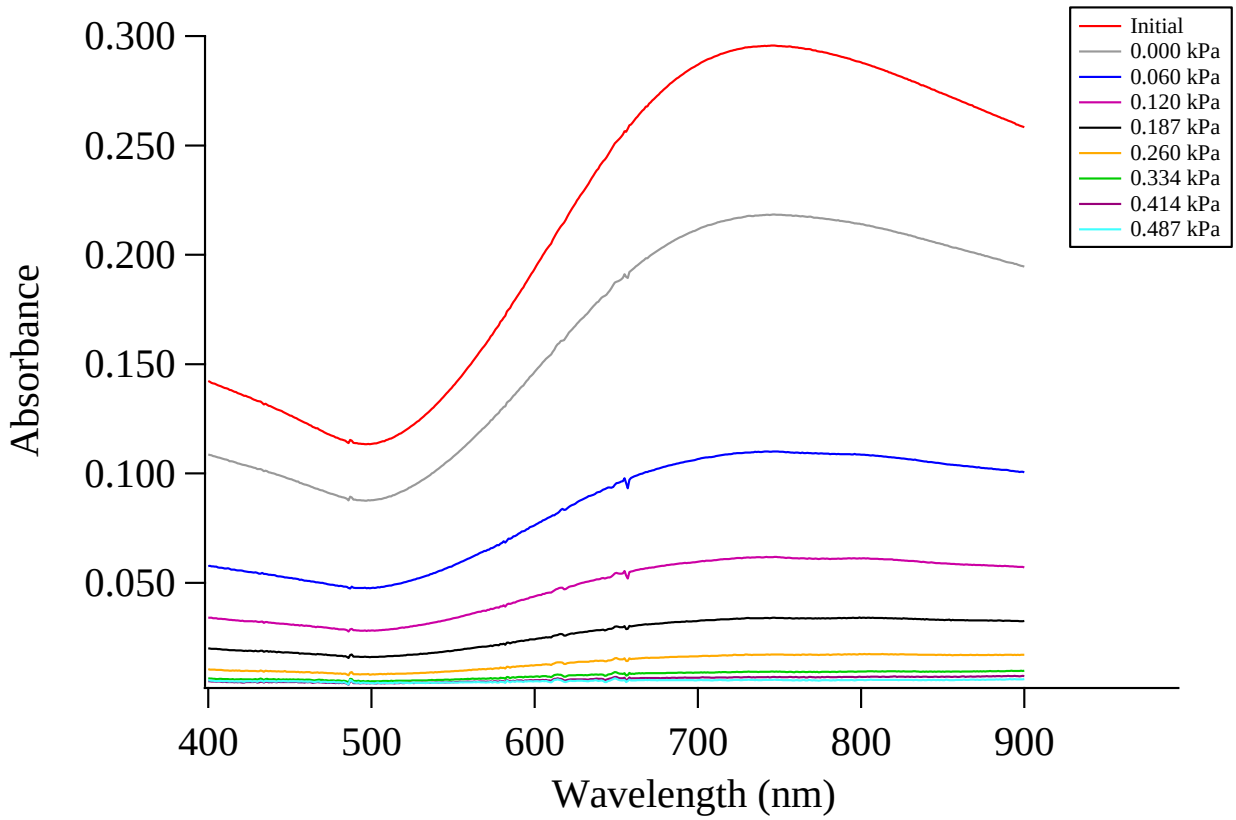

Figure 14. Absorbance spectra obtained while polishing an untreated Au-plated PMMA sample. The decrease in absorbance values in the 400 – 900 nm range corresponds to a decrease in the number of Au particles on the PMMA surface. The sample was polished until the spectrum leveled out at approximately zero absorbance units.

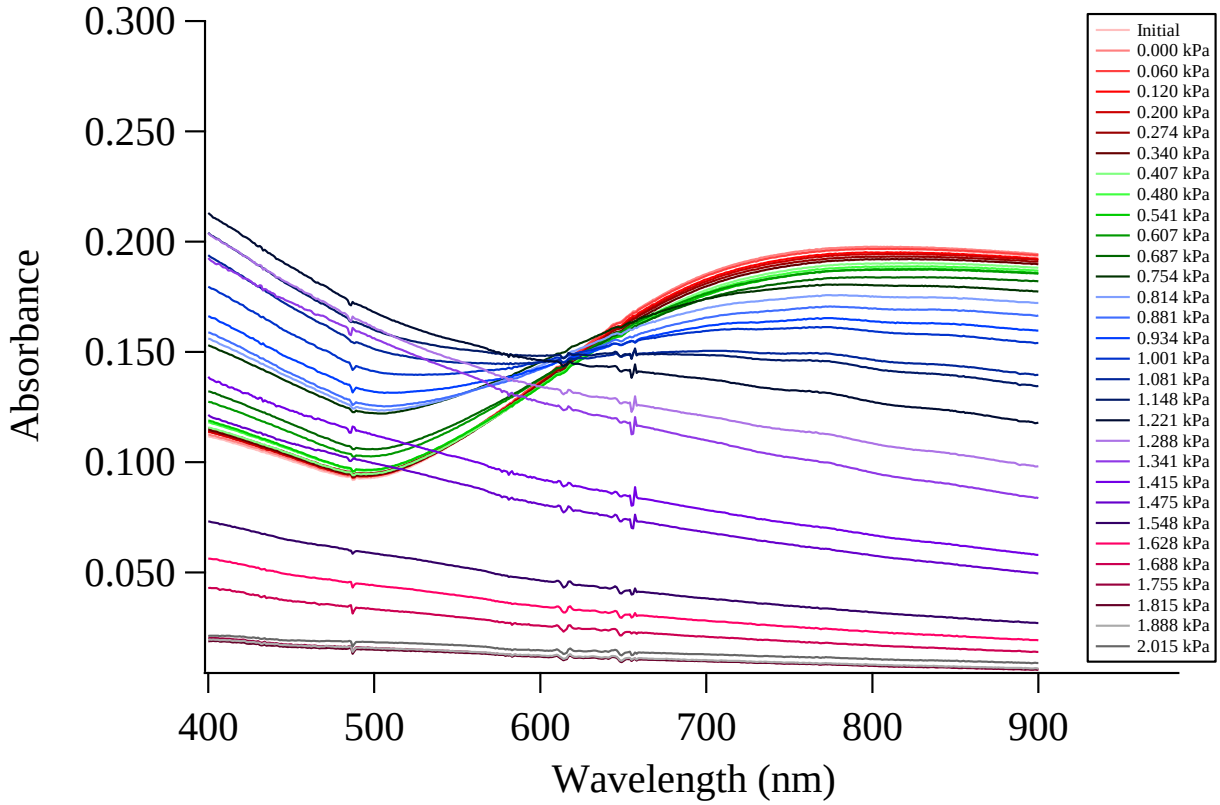

Figure 15. Absorbance spectra obtained during the polishing of a Au-plated PMMA sample exposed to heated $CHCl_3$ vapor following Au deposition.

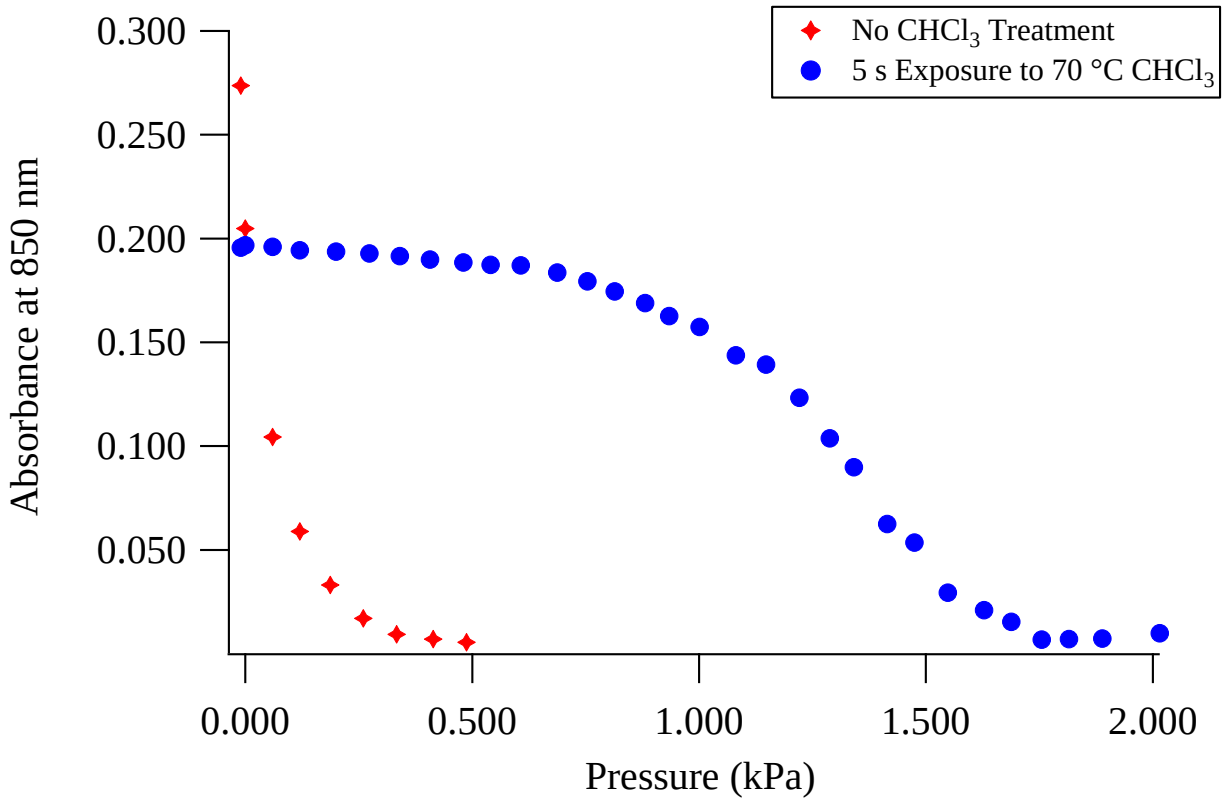

Figure 16. Comparison between the pressure required to remove the Au from a PMMA sample exposed to $CHCl_3$ vapor and the pressure required to remove the Au from an untreated substrate.

The average absorbance and standard deviation at 700 nm were calculated for five untreated Au-coated PMMA samples and six treated samples prior to any polishing (Supporting Information, Table S1) The pressure at which the first significant Au removal was observed (P_1) was defined as the pressure at which the absorbance was two standard deviations below the initial absorbance (Supporting Information, Table S2). The pressure at which the Au removal leveled off (P_2) was defined as the pressure at which the measured absorbance was two standard deviations above the final absorbance (Supporting Information, Table S2). P_1 and P_2 for the untreated sample were determined to be 0.000 ± 0.011 kPa and 0.144 ± 0.292 kPa, respectively (Supporting Information, Figure S4). P_1 and P_2 for the treated sample were calculated at 1.153 ±

0.222 kPa and 1.520 ± 0.221 kPa, respectively. Exposure to heated $CHCl_3$ following metal deposition increased P_1 by ~1.2 kPa and increased P_2 by nearly 1.4 kPa.

P_1 and P_2 values were calculated for six treated and five untreated samples polished using the first generation force-measuring device (Figures 17 and 18). While the difference in P_1 for treated versus untreated Au is statistically significant within reason, the results obtained for P_2 are not so conclusive. Statistical agreement among P_1 and P_2 calculations for a given sample type is observed only because the error bars are on the same order of magnitude as the actual values (Figures 17 and 18). The inconsistencies of these results can be attributed to an inherent design flaw in the force-measuring device. Because the device contains no mechanism for accurately determining "zero force," the initial application of force is not consistent across PMMA samples. The inability to polish each sample at the same starting point accounts for the imprecision associated with P_1 and P_2 values and severely limits the data acquisition method.

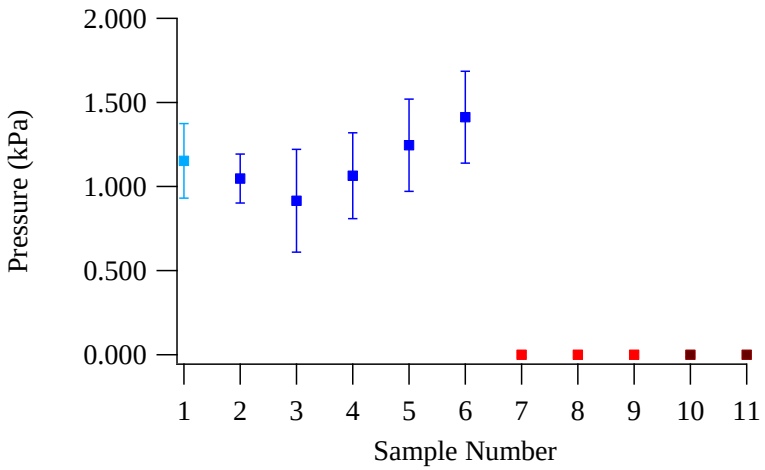

Figure 17. P_1 values obtained for post-treated samples (blue) and untreated Au-plated PMMA samples (red) using the first-generation force-measuring device. 60 Å of Au were deposited onto samples 1-11 using the same e-beam evaporation parameters. Samples 1-6 underwent the same $CHCl_3$ vapor exposure. Sample 1 and Samples 10-11 were polished after a modified spring system had been installed in the force-measuring device. The inconsistency in the initial force applied onto each sample accounts for the variability across treated P_1 values.

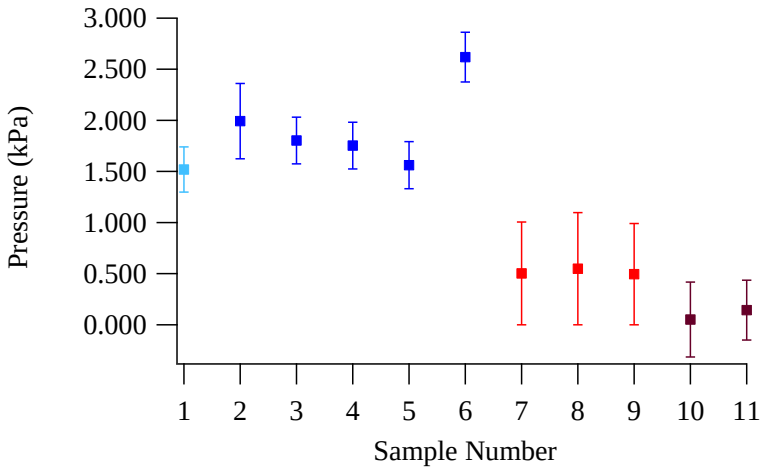

Figure 18. P_2 values obtained for post-treated samples (blue) and untreated Au-plated PMMA samples (red) using the first-generation force-measuring device. 60 Å of Au were deposited onto samples 1-11 using the same e-beam evaporation parameters. Samples 1-6 underwent the same $CHCl_3$ vapor exposure. Sample 1 and Samples 10-11 were polished after a modified spring system had been installed in the force-measuring device. The inconsistency in the initial force applied onto each sample accounts for the variability across both treated and untreated P_2 values. The formation of a cloudy residue on the PMMA surface following $CHCl_3$ exposure also contributes to the imprecision across treated P_2 values.

The use of e-beam evaporation to deposit the Au thin films also posed an issue for the data acquisition process. The use of high-energy electrons when depositing Au by e-beam inherently generates a significant amount of heat. The exact temperature inside the vacuum chamber cannot be easily controlled or determined, and modifying parameters such as deposition rate and delay time before deposition can vary the temperature during deposition. PMMA undergoes a glass transition from its solidified, semi-crystalline state to a more fluid phase at 105 °C, and if the temperature inside the vacuum chamber exceeds this value, the PMMA sample is subject to warping and discoloration. Warping induces light scattering, the spectroscopic effects of which are seen in Figure 15. Because the UV-VIS spectrophotometer outputs all non-

transmitted light as absorbance, any significant scattering is incorporated into the spectral pattern. A sudden "absorbance" increase in the 400-600 nm region corresponds to the application of 1.081 ± 0.011 kPa of pressure and can be attributed to the scattering of light by scratches on the sample surface. These scratches are induced by the torque (rotational force) applied onto the sample during polishing. This change in spectral pattern is not observed for untreated samples because the force required to scratch the sample surface exceeds that required to polish unexposed Au. Because this increase is not seen at 850 nm, scattering caused by polishing alone does not impede data acquisition when generating an absorbance-pressure curve. However, warping-induced scattering does affect the spectra around 850 nm, producing spectral patterns that suggest the absorbance actually increases with Au removal once a given pressure has been applied. This scattering effect makes it impossible to obtain accurate curves for Au-plated PMMA samples that have undergone $CHCl_3$ treatment.

Quantifying the effectiveness of $CHCl_3$ post-treatment using the second generation force-measuring device. The limitations associated with the first generation force-measuring device and e-beam evaporation necessitated both an improvement in device design and the use of a new metal deposition method. The calibration curve produced for the second generation force-measuring device is shown in Figure 16. The equation for the line of best fit was used to determine the pressure applied to every PMMA sample as a function of the voltage output of the force sensor. The line of best fit is given by Equation 7:

(7) $y = -93.323x + 21.765$

The mass associated with each force increment was calculated by substituting in the observed voltage for x. The y-intercept needed to correlate a mass of 0.0 g, and therefore a pressure of 0.000 kPa, to the initial voltage reading was calculated using Equation 8:

(8) $y - intercept = 0 - (V * m)$

Where 0 is the desired y value of 0.0 g, V is the initial voltage, and m is the slope of the mass-voltage calibration plot (Figure 19). Once the mass associated with each polishing process was known, the pressure (kPa) of each force increment was calculated using Equations 5 and 6.

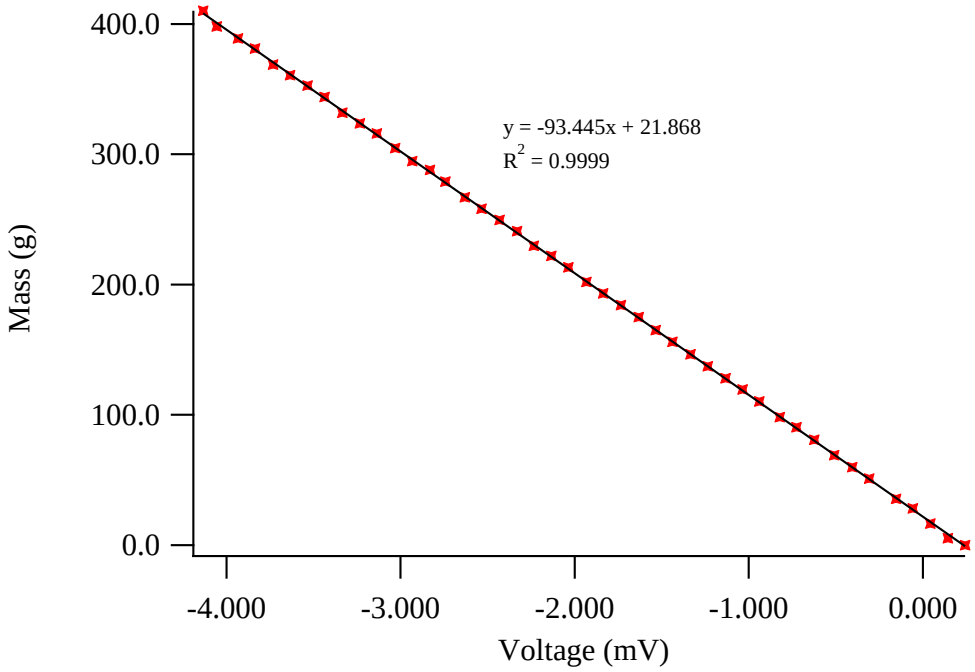

Figure 19. Calibration of the second generation force-measuring device. The slope of this linear fit and the slopes of two additonal calibration curves agree within error (Supporting Information, Figure S5).

The absorbance spectra obtained for each 20 s polishing process for an untreated sample are similar to those from samples polished with the first generation device and are displayed in Figures 20 and 21 for reference. Additional absorbance-pressure curves for untreated samples

can be found in the Supporting Information (Figure S6). The absorbance values at 850 nm were plotted as a function of applied polishing pressure to generate two comparative S-shaped curves (Figure 22). P_1 and P_2 were determined to be 0.000 ± 0.006 kPa and 0.675 ± 0.067 kPa for the untreated sample, respectively. P_1 and P_2 were determined to be 1.241 ± 0.029 kPa and 2.048 ± 0.021 kPa for the treated sample, respectively. Exposure to heated $CHCl_3$ following metal deposition was found to increase P_1 by ~1.2 kPa and P_2 by nearly 1.4 kPa.

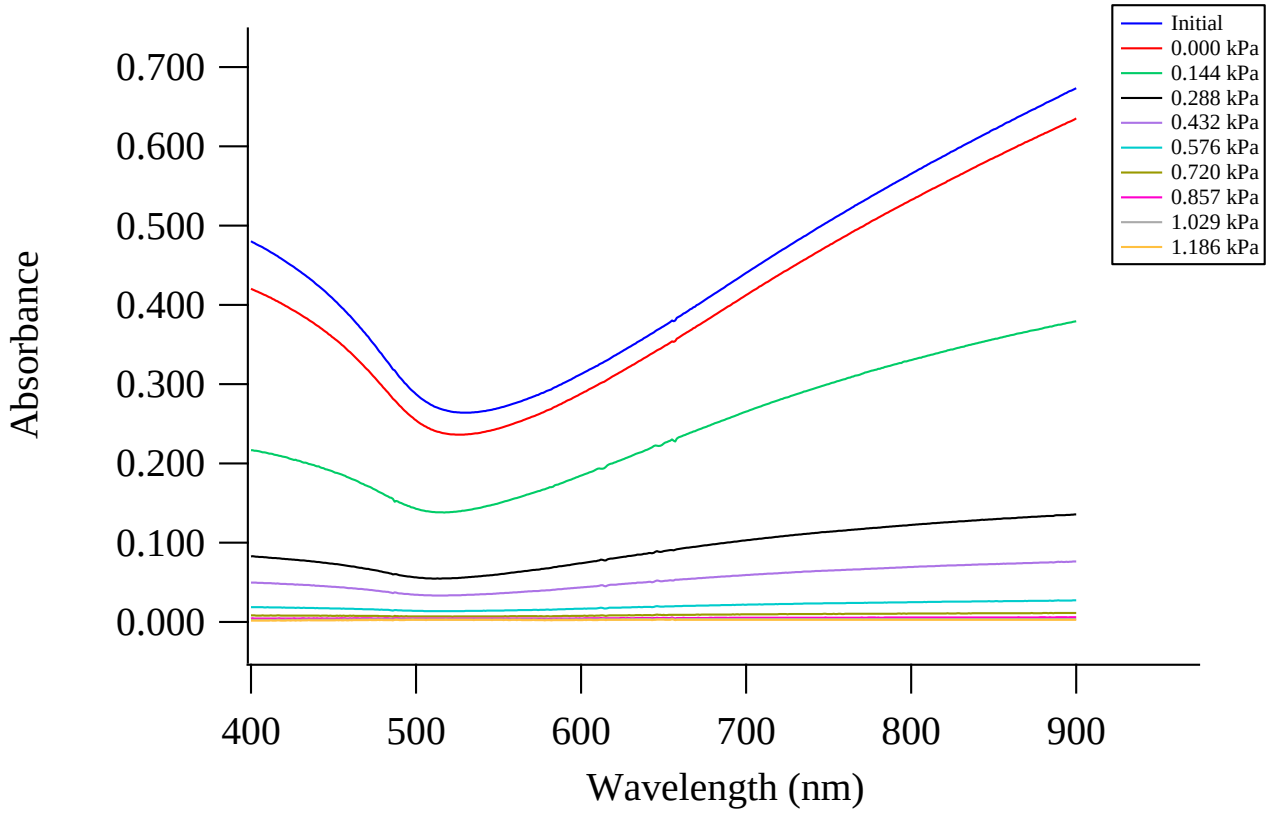

Figure 20. Absorbance spectra acquired for an untreated Au-plated PMMA sample. For generating the absorbance-pressure plot, the absorbance of light at 850 nm was chosen due to its proximity to the wavelength of maximum absorbance.

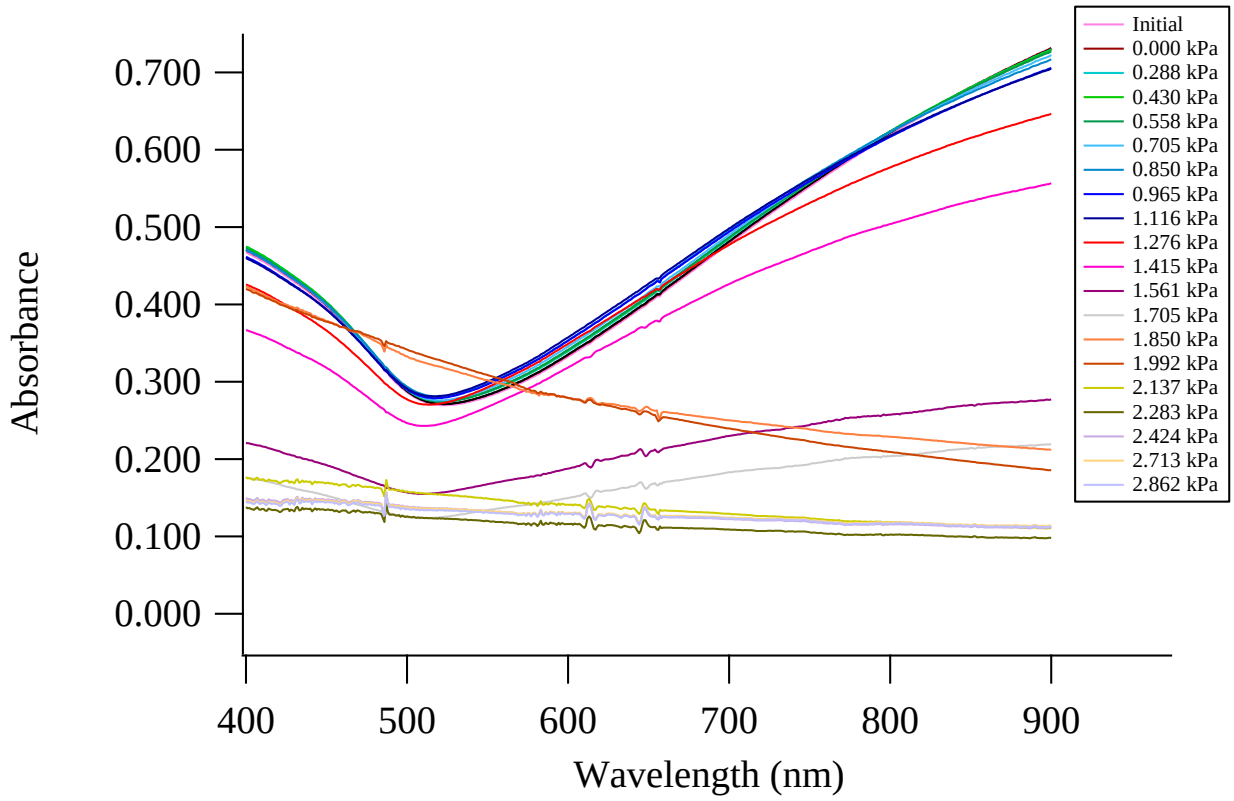

Figure 21. Absorbance spectra acquired for a Au-plated PMMA sample exposed to heated $CHCl_3$ vapor following Au deposition.

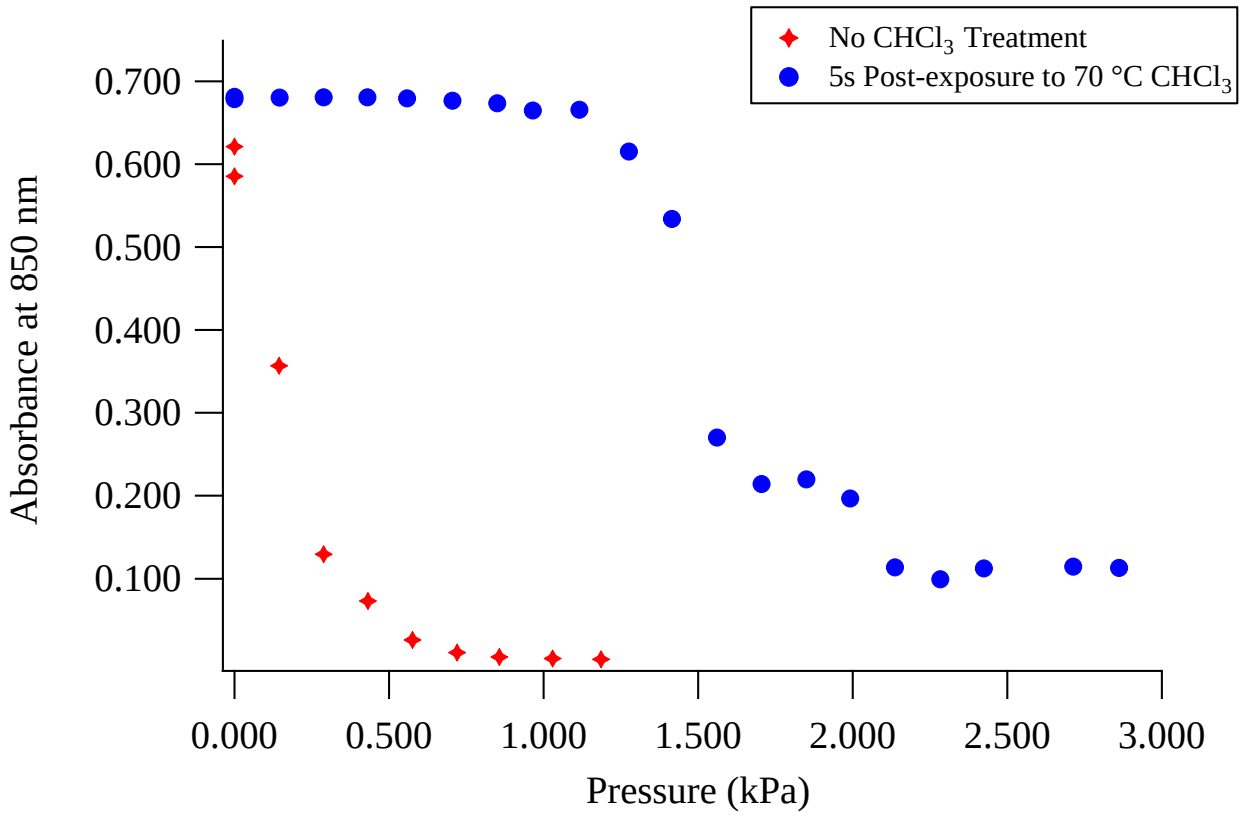

Figure 22. Comparison between the pressure required to remove the Au from a PMMA sample exposed to $CHCl_3$ vapor and the pressure required to remove the Au from an untreated substrate.

Using the second generation device in place of the first generation device reduces the percent error associated with each pressure by 1 order of magnitude, and there is still excellent statistical agreement among P_1 and P_2 values obtained for untreated samples (Figures 23 and 24). While the accuracy is still limited by the crude method of using human hearing to establish when the sample first touches the polishing pad, the precision in the zero force is improved due to the incorporation of a load cell into the design. A comparison between the calibration curves obtained for each force-measuring device also affirms the superiority of the second generation design. The acquisition of an R^2 value closer to 1 suggests a better linear fit and the range of

masses that can be accurately interpolated is increased by almost a factor of 3 (Supporting Information, Figures S1 and S4).

The use of magnetron sputtering deposition in place of e-beam evaporation complements the improvements produced from the second generation force-measuring device. Because the metal films deposited by this technique are not subjected to the high temperature environment associated with e-beam evaporation, the problematic warping-induced spectral effects are eliminated. A comparison between the standard deviation of the initial absorbance values for both treated and untreated Au-coated PMMA samples provides further support for using magnetron sputtering over e-beam evaporation (Supporting Information, Table S1). The standard deviations of the absorbance for unpolished Au thin films deposited by magnetron sputtering are significantly lower, suggesting that this technique deposits more uniform thin films than does e-beam evaporation.

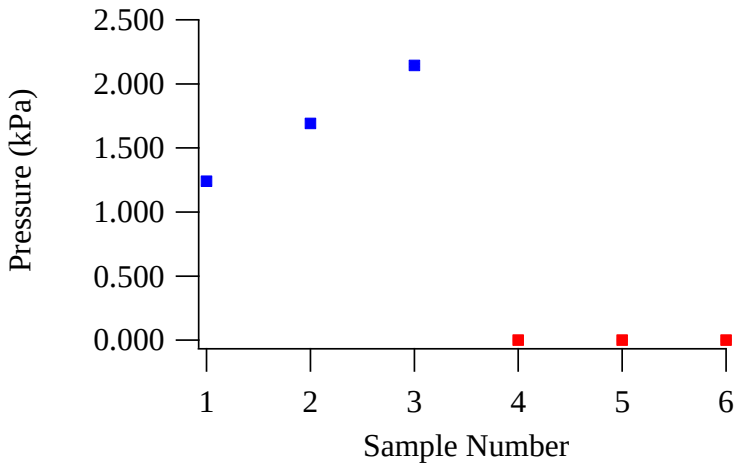

Figure 23. P_1 values obtained for post-treated samples (blue) and untreated Au-plated PMMA samples (red) using the second-generation force-measuring device. Au was deposited onto samples 1-6 using the same magnetron sputtering deposition parameters. Samples 1-3 underwent the same $CHCl_3$ vapor exposure. The inconsistency in the initial force applied onto each sample accounts for the variability across treated P_1 values. Because the percent error

of each treated P_1 value is on the order of 10^{-3} mV, the error bars are minuscule and cannot be seen with the naked eye.

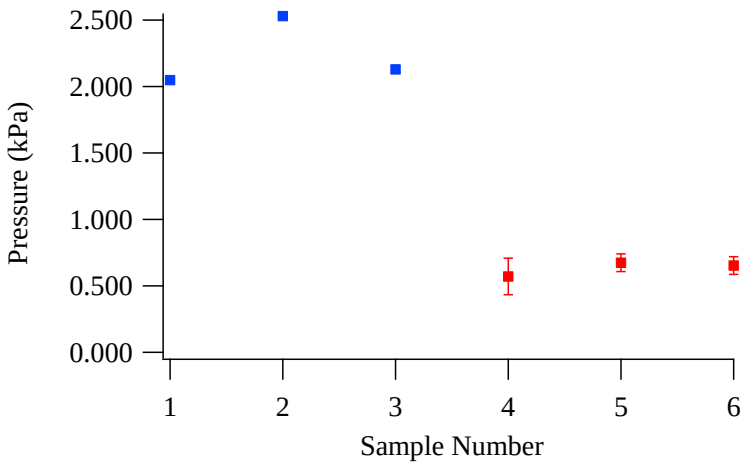

Figure 24. P_2 values obtained for post-treated samples (blue) and untreated Au-plated PMMA samples (red) using the second-generation force-measuring device. Au was deposited onto samples 1-6 using the same magnetron sputtering deposition parameters. Samples 1-3 underwent the same $CHCl_3$ vapor exposure. The inconsistency in the initial force applied onto each sample accounts for the variability across both treated and untreated P_2 values. The formation of a cloudy residue on the PMMA surface following $CHCl_3$ exposure also contributes to the imprecision across treated P_2 values. Because the percent error of each treated P_2 value is on the order of 10^{-3} mV, the error bars are minuscule and cannot be seen with the naked eye. The error bars for the untreated P_2 values are on the order of 10^{-2} mV and are therefore more visible.

A significant limitation seen in the new method is the fact that the pressure calculations among different post-treated samples do not agree within error. A comparison between the absorbance-pressure curves of the three samples clearly indicate the source of the discrepancy (Figure 25). The most prominent factor contributing to this inconsistency is the unevenness of the PMMA surface arising from the manufacturing process. This induces an uneven polishing of the PMMA surface across different samples, which in turn varies the quantity of Au being removed from the area through which light from the UV-VIS source is transmitted. In the future,

developing a method for planarizing the PMMA surface, potentially through polishing, will alleviate this issue. The formation of a light-absorbing cloudy residue whose consistency varies from sample to sample also inhibits data acquisition. In fact, the difficulty of removing this residue prevents the complete polishing of the sample surface with respect to the PMMA blank. The agreement of P_1 and P_2 values among the untreated samples indicate that the aforementioned complications are specific to $CHCl_3$-exposed samples. A final consideration is the 25% variation seen in the thickness of the Au thin films deposited by magnetron sputtering (140.7 ± 34.8 Å). During a metal deposition, the sample holder rotates to maximize the uniformity of the films. On a single PMMA surface, the thickness of deposited Au will vary based on its distance from the center of the rotary holder. To ensure consistency of the thin films across samples, the PMMA squares are placed in the same three or four sample positions closest to the center. During UV-VIS spectra acquisition, situating each Au-plated sample in the exact same location of the sample holder ensures that the light passes through the same area of every PMMA sample. Implementing the two aforementioned procedures should minimize any quantitative discrepancies resulting from an uneven Au film.

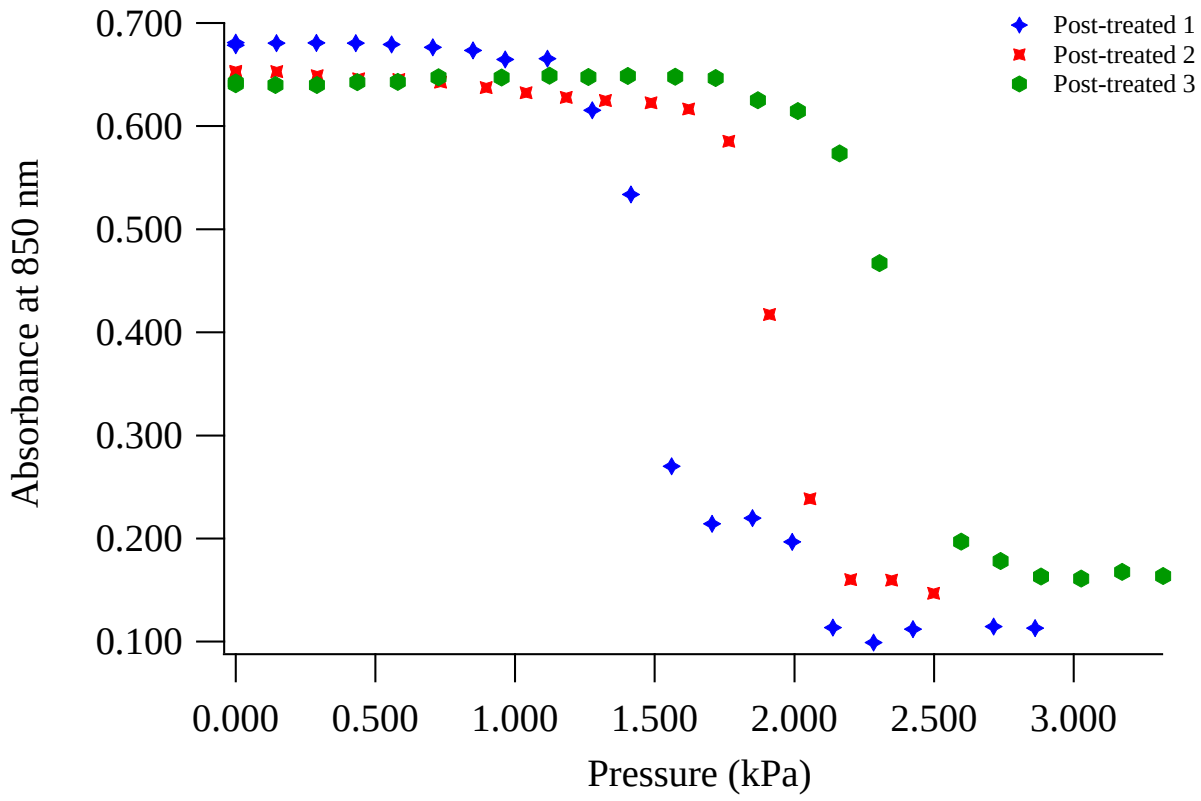

Figure 25. Absorbance-pressure curves generated for post-treated Au-plated PMMA samples using the second generation force-measuring device. Au was deposited onto all samples using the same magnetron sputtering deposition parameters. The samples also underwent the same $CHCl_3$ vapor exposure. The inconsistency in the initial force applied onto each sample, the formation of a cloudy residue on the PMMA surface following $CHCl_3$ exposure, and the uneven surface of each sample account for the observed variability.

Characterization of a Au-plated PMMA surface exposed to $CHCl_3$. AFM images showing Treated Sample 6 during different stages of the polishing process provide insight into the mechanism behind the effectiveness of $CHCl_3$ treatment. Due to time constraints, AFM data showing the entire Au removal procedure were only obtained for one sample.

Figure 26a depicts a clear image of a separate, untreated Au-plated sample. The consistency in surface feature height (typically in the 50.0 nm range) across the image indicates

an even surface. By contrast, the exposure of Treated Sample 6 to $CHCl_3$ vapor and subsequent initial polishing yields a blurry image in which the surface height varies from ~ 0.0 – 75.0 nm (Figure 26b). Additional Au-plated and blank PMMA surfaces were exposed to $CHCl_3$ vapor, and because the AFM images for these samples also appeared blurry, it was concluded that $CHCl_3$ vapor exposure induces the formation of a cloudy residual layer. Upon polishing with 1.596 ± 0.015 kPa of pressure, the gradual removal of the cloudy layer is observed (Figure 26c). Scratches induced by the circular motion of the polishing wheel are also apparent, and the larger range of feature heights (~ 0.0 – 200.0 nm) indicates a roughening of the PMMA surface. The final AFM image for Treated Sample 6 was acquired after the sample was polished with 2.861 ± 0.016 kPa of pressure (Figure 26d). Additional scratching is observed, and virtually all of the cloudy layer has been removed.

The cloudy residue formed during $CHCl_3$ vapor exposure may provide insight into the mechanism behind the efficacy of $CHCl_3$ post-treatment (Figure 4). Because the cloudy layer was observed on both Au-plated and blank PMMA surfaces, it may correspond to the formation of the Lewis acid-base adduct between the PMMA and the $CHCl_3$ (Figure 4a). When a Au atom enters the pocket created by the adduct and inserts itself into a C-Cl bond, a residual $CHCl_3$ radical is formed (Figure 4b-c). The subsequent behavior of this radical remains unsolved, and the cloudy residue may provide an answer. Future work will utilize spectroscopy to study the elemental composition of this residue in hopes of elucidating its nature.

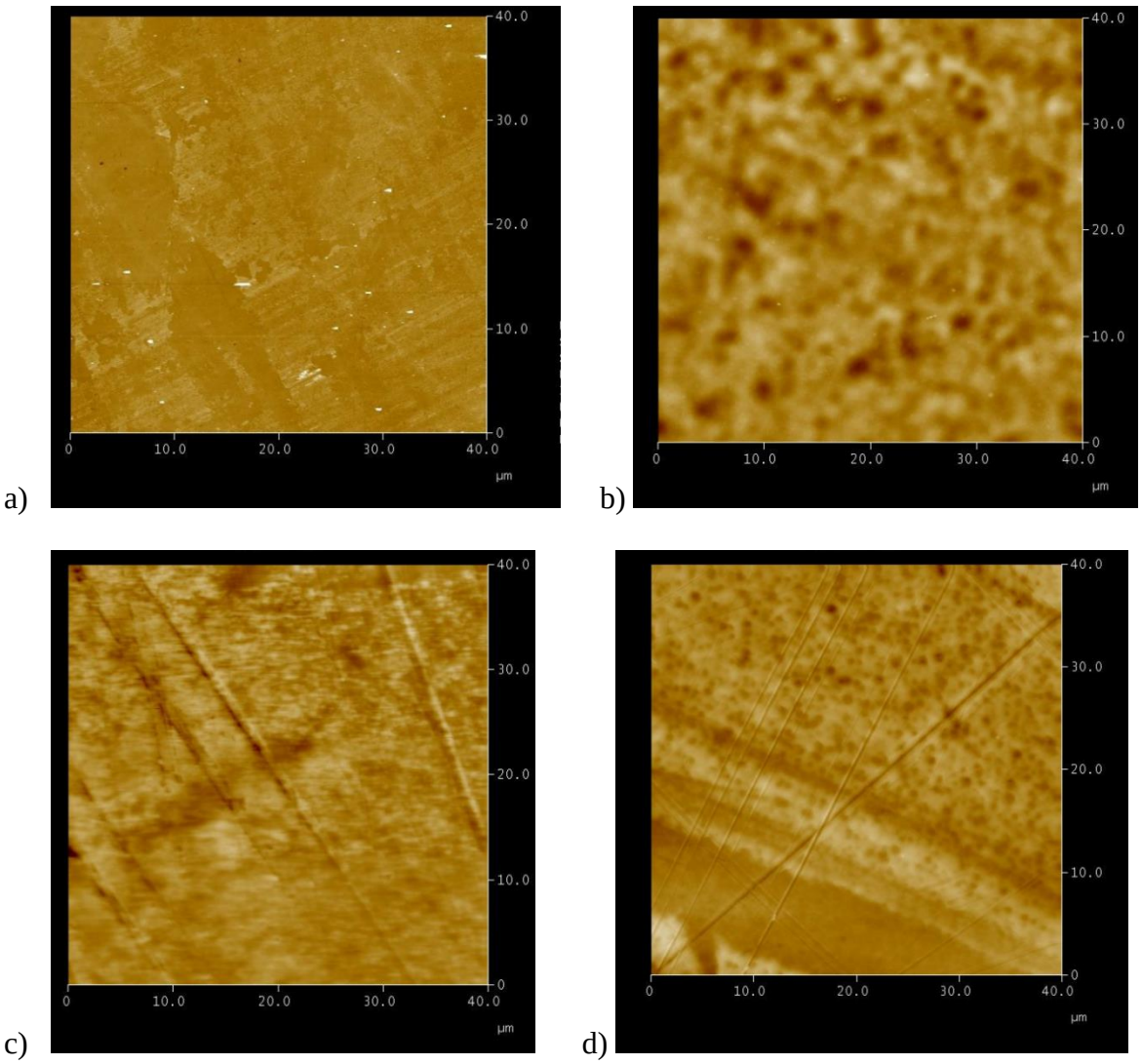

Figure 26. AFM images depicting the $CHCl_3$ vapor exposure and polishing processes. a) Au-plated PMMA square that has not been exposed to $CHCl_3$ vapor. b) Au-plated sample exposed to heated $CHCl_3$ vapor and polished with roughly 0 kPa of applied pressure. c) Vapor-exposed Au-plated sample polished with 1.596 ± 0.015 kPa of pressure. d) Vapor-exposed PMMA sample polished with 2.861 ± 0.016 kPa of pressure.

Comparison between $CHCl_3$ pre-treatment and post-treatment. Figure 27 depicts the pressure required to remove Au from a PMMA sample exposed to $CHCl_3$ vapor prior to metal deposition. At this time, a full evaluation of the data comparing $CHCl_3$ pre-treatment and post-

treatment has not been generated, but the pressure-absorbance curves do yield some interesting qualitative observations. A steep drop-off is observed for the pre-treatment, indicating the quick removal of the outermost Au atoms. For a post-treated sample, the first significant Au removal requires the application of nearly 1.500 kPa of pressure. Despite the differences in initial Au removal, the leveling out of the absorbance spectra for both pre-treated and post-treated samples occurs following the application of ~ 3.000 kPa of pressure.

For the pre-treated sample, this result agrees with the proposed mechanism for how $CHCl_3$ vapor exposure improves Au-PMMA adhesion (Figure 4). If the PMMA surface is chemically activated prior to metal deposition, then the Au atoms that insert themselves into the PMMA-$CHCl_3$ binding pocket first will best adhere to the surface, explaining the quick removal of the upper Au layer. The reason behind the slow removal of Au atoms from the post-treated surface remains unclear. One hypothesis suggests that the surface PMMA seeps up over the Au upon being softened by the $CHCl_3$ vapor. The uppermost Au atoms then insert themselves into the PMMA-$CHCl_3$ binding pockets and resist removal by polishing. Further study will utilize techniques such as Time-of-Flight Secondary Ion Mass Spectrometry (TOF-SIMS) to test this hypothesis, and different thicknesses of Au thin films will undergo testing to determine whether film thickness affects the efficacy of pre-treatment versus post-treatment.

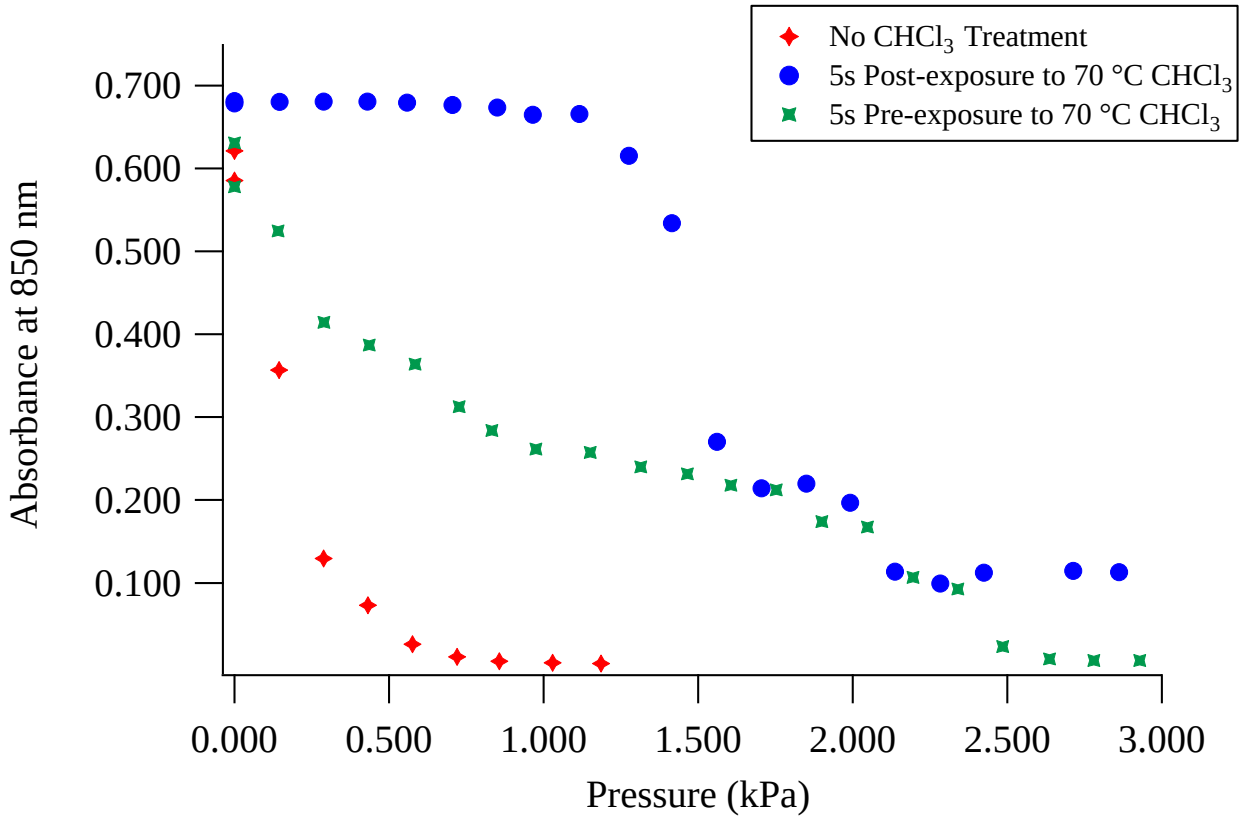

Figure 27. Comparison between the pressure required to remove the Au from a PMMA sample exposed to $CHCl_3$ vapor following deposition (blue), the pressure required to remove the Au from an untreated substrate (red), and the pressure required to remove the Au from a PMMA sample exposed to $CHCl_3$ vapor before deposition (green). All pressure measurements were obtained using the second-generation force-measuring device.

Selective Patterning. In addition to improving the adhesion of bulk Au films onto PMMA, post-deposition $CHCl_3$ vapor exposure can be used to allow millimeter-scale Au patterns to stick to a surface. Selective patterning encompasses the design and transfer of patterns onto a variety of different substrates and is important to the field of microfabrication (the assembly of small structures and devices).[18] Materials used in microfabrication processes are chosen for their desirable thermal, electrical, and optical properties pertaining to certain design requirements. Because selective patterning provides control over the shape, size, and position of nano- and microstructures composed of these materials,[19] it is useful in a variety of

technological applications including flexible electronics,[21] pixel device displays,[20] sensors,[21] and microfluidic[20] devices used in biomedical studies.

A series of 140.7 ± 34.8 Å thick Au thin films were selectively patterned onto PMMA (Figure 28). The particular selective patterning procedure presented in Scheme 1 is a simple modification of the post-metallization $CHCl_3$ vapor exposure. While only features on a mm-scale have been obtained, this work paves the way for utilizing $CHCl_3$ post-treatment to generate microscale patterns.

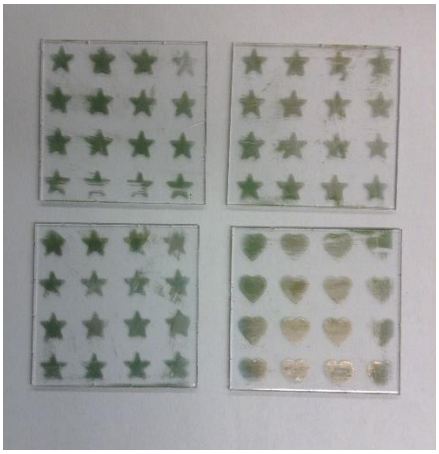

Figure 28. 140.7 ± 34.8 Å thick Au thin films patterned by post-deposition $CHCl_3$ vapor exposure.

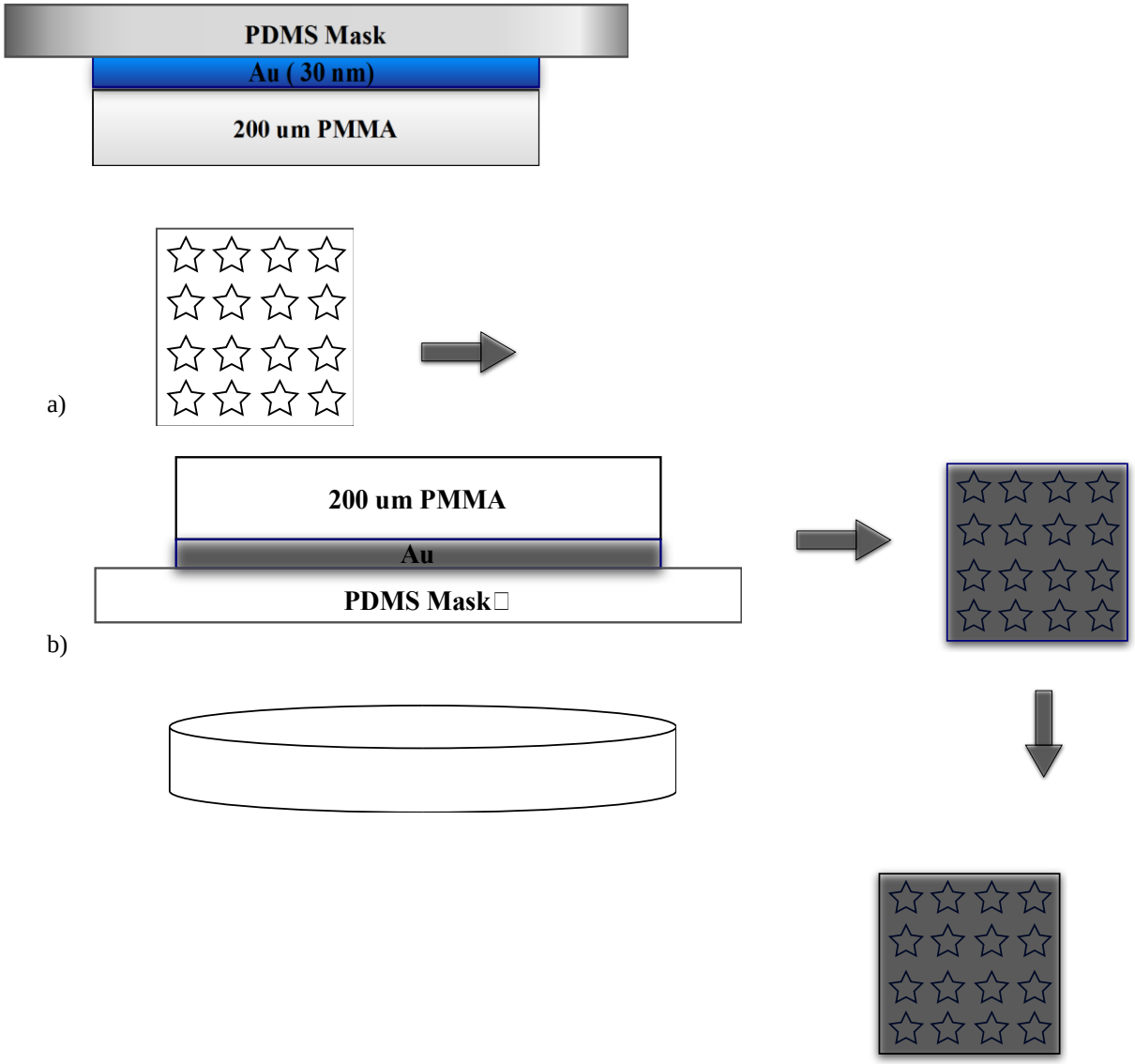

Scheme 1. Selective patterning process. a) Au is deposited onto a 200 μm thick PMMA sample and covered with a patterned PDMS mask. b) The Au-plated PMMA surface is exposed to heated $CHCl_3$ vapor through the mask. The $CHCl_3$ only reaches the star-shaped patterns. The sample is then wiped clean with a KimWipe to remove the untreated Au from the sample surface.

Conclusions

In conclusion, a reproducible and reliable quantitative method for measuring the effect of $CHCl_3$ vapor exposure in improving the adhesion of Au thin films onto PMMA has been developed and implemented. Using a specially designed force-measuring device, the percent error associated with each pressure measurement was on the order of 10^{-2} kPa. While the P_1 and P_2 values among untreated samples agreed within error, the same could not be said for treated samples due to such factors as uneven polishing and the formation of a cloudy residue that affected spectral patterns. $CHCl_3$ vapor exposure increased the amount of pressure required to remove Au from the PMMA surface by ~1.5 kPa (a 33% improvement), indicating that post-treatment does in fact improve adhesion at the Au-PMMA interface. A comparison between pre-treatment and post-treatment for 140.7 ± 34.8 Å thick Au thin films shows a more immediate removal of the Au for the pre-treated sample but indicates that it takes roughly the same amount of pressure to remove all of the Au from both samples. AFM data suggest that the reaction between the PMMA surface and $CHCl_3$ vapor yields a cloudy layer that is gradually removed during polishing. While this transformation has not yet been studied extensively, it may provide mechanistic insight into the vapor exposure process. The study of this cloudy layer and its implications will require spectroscopic studies such as XPS. In addition, selective patterning experiments have shown that $CHCl_3$ post-treatment can be utilized to deposit Au onto specific areas of a given sample.

Future work will focus on exposing Au-plated PMMA samples to $CHCl_3$ vapor at varying temperatures with different exposure times in order to optimize Au-PMMA adhesion. Further study will also concern the viability of post-treatment and pre-treatment as a function of Au film thickness. Finally, the newly developed quantitative method will be used to conduct adhesion

studies concerning different noble metals deposited onto PMMA, additional organic polar solvents, and plastics that are structurally similar to PMMA.

References

1. Mo, A. K.; Brown, V. L.; Rugg, B. K.; Devore, T. C.; Meyer, H. M.; Hu, X.; Hughes, W. C.; Augustine, B. H. Understanding the mechanism of solvent-mediated adhesion of vacuum deposited Au and Pt thin films onto PMMA substrates. *Adv. Funct. Mater.* **2013**, *23*, 1431-1439. DOI: 10.1002/adfm.201201955.
2. Li, W. T.; Charters, R. B.; Luther-Davies, B.; Mar, L. Significant improvement of adhesion between gold thin films and a polymer. *Appl. Surf. Sci.* **2004**, *233*, 227-233. DOI: 10.1016/j.apsusc.2004.03.220.
3. Mo, A. K.; Devore, T. C.; Augustine, B. H.; Zungu, V. P.; Lee, L. L.; Hughes, W. C. Improving the adhesion of Au thin films onto poly(methyl methacrylate) substrates using spun-cast organic solvents. *J. Vac. Sci. Technol., A.* **2011**, *29*. DOI: 10.1116/1.3562167.
4. Grace, J. M.; Gerenser, L. J. Plasma treatment of polymers. *J. Dispersion Sci. Technol.* **2003**, *24*, 305-341. DOI: 10.1081/DIS-120021793.
5. Hegemann, D.; Brunner, H.; Oehr, C. Plasma treatment of polymers for surface and adhesion improvement. *Nucl. Instrum. Methods Phys. Res., Sect. B.* **2003**, *208*, 281-286. DOI: 10.1016/S0168-583X(03)00644-X.
6. Arif, S.; Rafique, M. S.; Saleemi, F.; Sagheer, R.; Naab, F.; Toader, O.; Mahmood, A.; Rashid, R.; Mahmood, M. Influence of 400 keV carbon ion implantation on structural, optical, and electrical properties of PMMA. *Nucl. Instrum. Meth. B.* **2015**, *358*, 236-244.
7. Rabiatul, A. R.; Lokanathan, Y.; Rohaina, C. M.; Chowdhury, S. R.; Aminuddin, B. S.; Ruszymah, B. H. I. Surface modification of electrospun poly(methyl methacrylate) (PMMA) nanofibers for the development of in vitro respiratory epithelium model. *J. Biomater. Sci. Polym. Ed*. **2015**, *26*, 1297-1311.

8. Abrisa Technologies. Physical Vapor Deposition – Sputtering vs. Electron Beam Evaporation. http://abrisatechnologies.com/2012/09/physical-vapor-deposition-sputtering-vs-electron-beam-evaporation/ (accessed Jan 31, 2016).
9. Raimondo, T.; Puckett, S.; Webster, T.J. Greater osteoblast and endothelial cell adhesion on nanostructured polyethylene and titanium. *Int. J. Nanomedicine*. **2010**, *5*, 647-652. DOI: 10.2147/IJN.S13047.
10. Angstrom Engineering. Electron Beam Evaporation. http://angstromengineering.com/tech/electron-beam-evaporation/ (accessed Jan 31, 2016).
11. FerroTec. Electron Beam Evaporation. http://angstromengineering.com/tech/electron-beam-evaporation/ (accessed Jan 31, 2016).
12. Angstrom Sciences. Magnetron Sputtering. http://www.angstromsciences.com/magnetron-sputtering-deposition (accessed Jan 31, 2016).
13. Mo, A. K. (2010). *Understanding the Role of Solvents in the Adhesion of Au Thin-Films onto PMMA* [PowerPoint slides].
14. Omega. Load Cell. http://www.omega.com/prodinfo/loadcells.html (accessed Feb 13, 2016).
15. nanoComposix. Characterization Techniques. http://nanocomposix.com/pages/characterization-techniques (accessed Feb 29, 2016).

16. Michigan State University. Visible and Ultraviolet Spectroscopy. http://www2.chemistry.msu.edu/faculty/reusch/VirtTxtJml/Spectrpy/UV-Vis/spectrum.htm (accessed Jan 28, 2016).
17. Michigan State University. UV-Visible Spectroscopy. http://www2.chemistry.msu.edu/faculty/reusch/VirtTxtJml/Spectrpy/UV-Vis/uvspec.htm#uv1 (accessed Jan 28, 2016).
18. Xia, Y.; Whitesides, G. M. Soft lithography. *Angew. Chem. Int. Ed.* **1998**, *37*, 550-575. DOI: 10.1002/(SICI)1521-3773(19980316)37:5<550::AID-ANIE550>3.0.CO;2-G.
19. Smythe, E. J.; Dickey, M. D.; Whitesides, G. M.; Capasso, F. A technique to transfer metallic nanoscale patterns to small and non-planar surfaces. *ACS Nano.* **2009**, *3*, 59-65. DOI:10.1021/nn800720r.
20. Wang, W.; Cheng, Z.; Yang, P.; Hou, Z.; Li, C.; Li, G.; Dai, Y.; Lin, J. Patterning of YVO_4:Eu^{3+} luminescent films by soft lithography. *Adv. Funct. Mater.* **2011**, *21*, 456-463. DOI: 10.1002/adfm.201001467.
21. Cai, X.; Wang, Y.; Wang, X.; Ji, J.; Hong, J.; Pan, F.; Chen, J.; Xue, M. Fabrication of ultrafine soft-matter arrays by selective contact thermochemical reaction. *Sci. Rep.* **2013**, *3*, 1780. DOI:10.1038/srep01780.

Appendix: Supporting Information

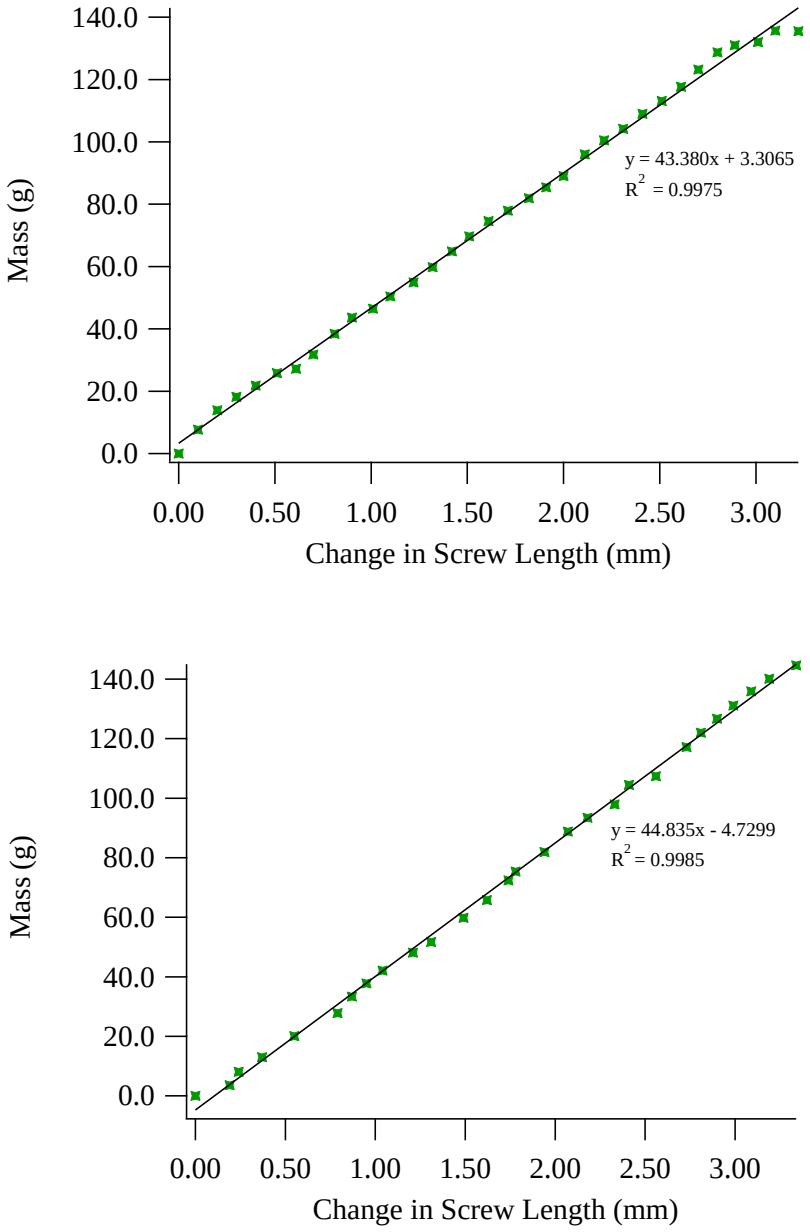

Figure S1. Calibration curves generated for the first generation force-measuring device following the incorporation of a modified spring system. These two curves were combined to construct the plot presented in Figure 13.

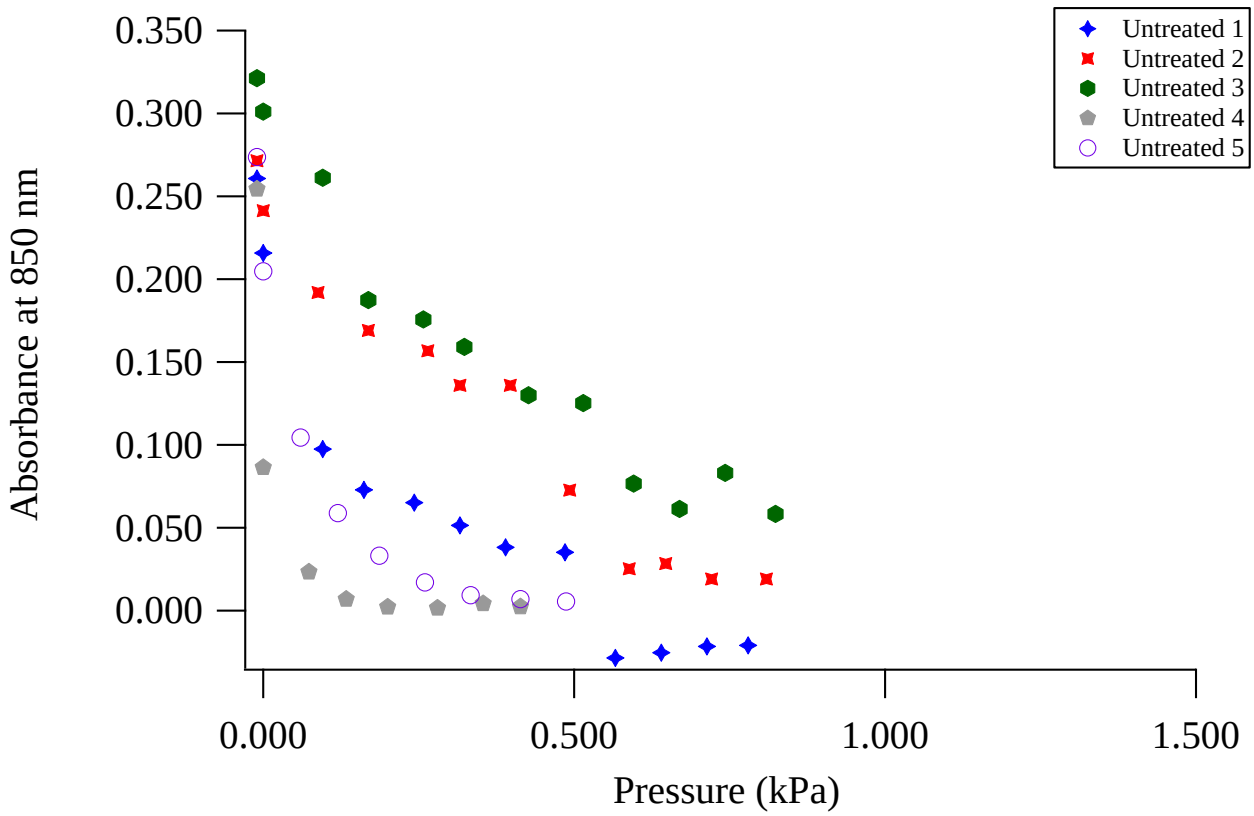

Figure S2. Absorbance-pressure curves generated for untreated Au-plated PMMA samples using the first generation force-measuring device. Data for untreated samples 4 and 5 were obtained following the incorporation of the modfied spring system into the device. Because the results obtained with the modified spring were deemed to be more precise, untreated sample 4 was chosen to be shown in Figure 14. 60 Å of Au were deposited onto all samples at a rate of 2 Å /s using e-beam evaporation. The inconsistency in the initial force applied onto each sample accounts for the variability between curves.

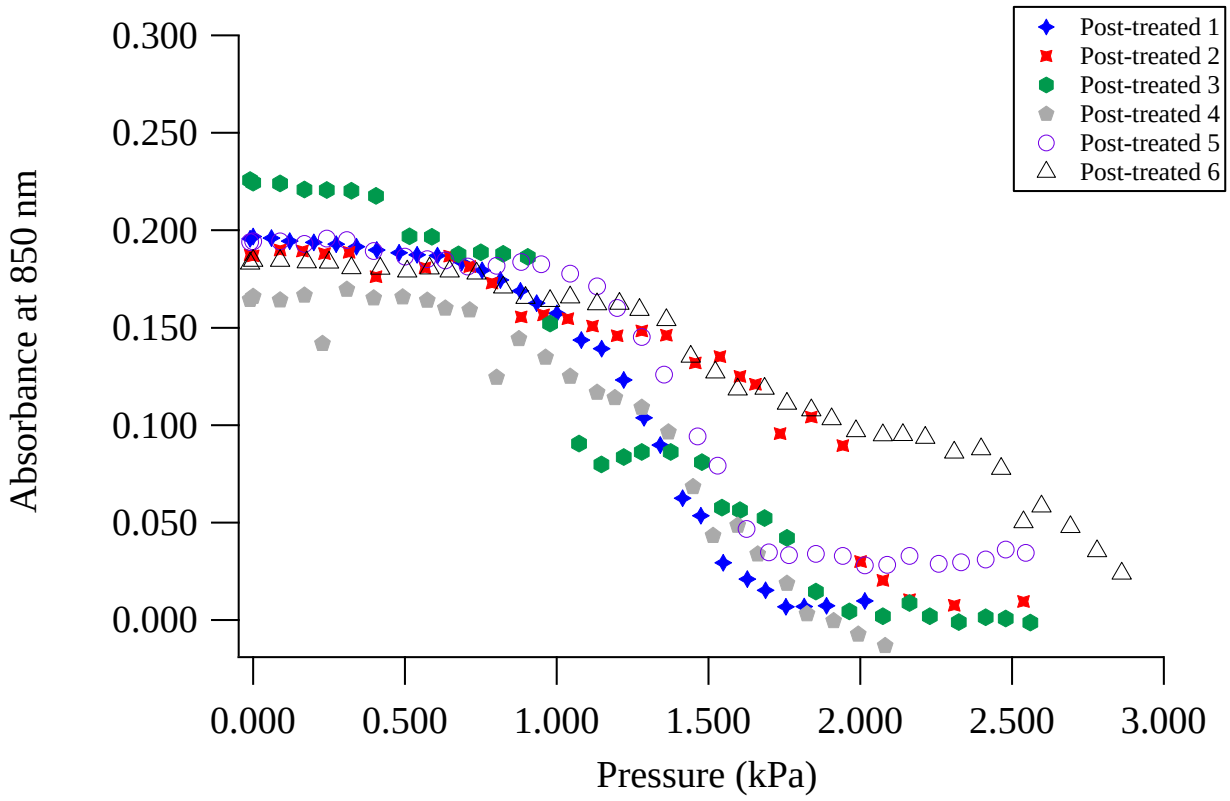

Figure S3. Absorbance-pressure curves generated for post-treated Au-plated PMMA samples using the first generation force-measuring device. The data for treated sample 1 were obtained following the incorporation of the modfied spring system into the device. Sample 1 is presented in Figure 15. Because the results obtained with the modified spring were deemed to be more precise, treated sample 1 was chosen to be shown in Figure 15. 60 Å of Au were deposited onto all samples at a rate of 2 Å /s using e-beam evaporation. All samples were exposed for 5 s to $CHCl_3$ vapor heated at 70 °C for 10 minutes. The inconsistency in the initial force applied onto each sample and the formation of a cloudy residue on the PMMA surface following $CHCl_3$ exposure accounts for the variability between curves.

Error Calculations

The resolution of the UV-VIS spectrophotometer yielded a standard deivation on the order of 10^{-5} for each absorbance value, rendering the error negligible. The following equation was used to calculate the percent error associated with each pressure:

$$(S1) \quad \%Error = \left(\frac{Error\ D}{D}\right) + \left(\frac{Error\ m}{m}\right)$$

where D is the caliper reading, Error D is the error associated with the caliper reading, m is the slope of the calibration curve used to calculate the pressure for a given force increment, and Error m is the error associated with the slope. For the second generation device, the voltage reading and associated error were used in place of distance measurements. The slope of the calibration curve generated for the unmodified first generation force-measuring device was determined to be 48.392 ± 0.705 kPa^{-1}. The slope of the calibration curve obtained after installing the modified spring system was 43.885 ± 0.46 kPa^{-1}. The slope of the best linear fit for the second generation device was determined to be -93.323 ± 0.142 kPa^{-1}.

Pressure 1 and 2 Calcuations

Second generation device				**First generation device**			
Untreated		Treated		Untreated		Treated	
1	0.608	1	0.697	1	0.279	1	0.182
2	0.621	2	0.724	2	0.286	2	0.264
3	0.614	3	0.684	3	0.334	3	0.213
Average:	0.614	4	0.703	4	0.306	4	0.159
1 SD	0.007	5	0.697	5	0.287	5	0.184
2 SD	**0.013**	6	0.704	**Average:**	0.298	6	0.167
		7	0.716	**1 SD**	0.022	7	0.185
		8	0.678	**2 SD**	**0.045**	**Average:**	0.193
		9	0.642			**1 SD**	0.036
		10	0.653			**2 SD**	**0.071**
		Average:	0.690				
		1 SD	0.026				
		2 SD	**0.052**				

Table S1. Average absorbance and standard deviation at 700 nm (first generation device) and 850 nm (second generation device) for a series of unpolished Au-plated PMMA samples. 60 Å of Au was deposited via e-beam evaporation onto the samples polished using the first generation force-measuring device. 140.7 ± 34.8 Å of Au was deposited via magnetron sputtering onto the samples polished using the second generation force-measuring device.

Absorbance	Pressure (kPa)
0.678	N/A
0.681	0.000
0.680	0.146
0.681	0.288
0.681	0.430
0.679	0.558
0.677	0.705
0.674	0.850
0.665	0.965
0.666	1.116
0.615	1.276
0.534	1.415
0.270	1.561
0.214	1.705
0.220	1.850
0.197	1.992
0.114	2.137
0.099	2.283
0.112	2.424
0.114	2.713
0.113	2.862

Table S2. Absorbance at 850 nm and corresponding pressure for second generation treated sample 1. Two standard deviations from the mean was determined to be ± 0.052 absorbance units for unpolished, $CHCl_3$-exposed Au thin films that were 140.7 ± 34.8 Å thick. P_1 was calculated by first subtracting 0.052 from the initial absorbance to yield an absorbance of 0.626. The absorbance measurements between which this value fell and the corresponding pressure (highlighted in red) were used to find P_1 via linear interpolation. P_2 was calculated by first adding 0.052 to the final absorbance measurement to yield a value of 0.165. The absorbance measurments between which this value fell and the corresponding pressure (highlighted in blue) were used to find P_2 via linear interpolation.

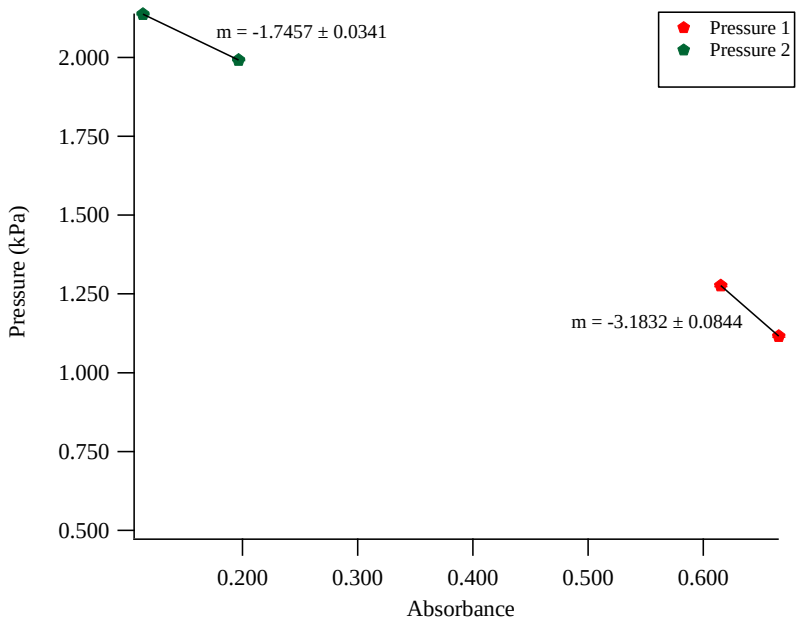

Figure S4. Linear interpolation between two points to calculate P_1 (red) and P_2 (green).

The slopes acquired in Figure S4 were used to calculate P_1 and P_2 using the point-slope formula:

$$(S2) \quad y - y1 = m * (x - x1)$$

where y1 and x1 are one of the absorbance-pressure pairs used in the interpolation (Table S2), m is the slope, x is the absorbance that is two standard deviations below the initial value (P_1) or two standard deviations above the final measurement (P_2), and y is the pressure being solved. The error associated with P_1 or P_2 is calculated using the following equation:

$$(S3) \quad Error = \left(\frac{Error\ m}{m}\right) + \left(\frac{Error\ P}{P}\right)$$

where m is the slope, Error m is the associated error, P is the calculated P_1 or P_2 value, and Error P is the associated error calculated using Equation S1.

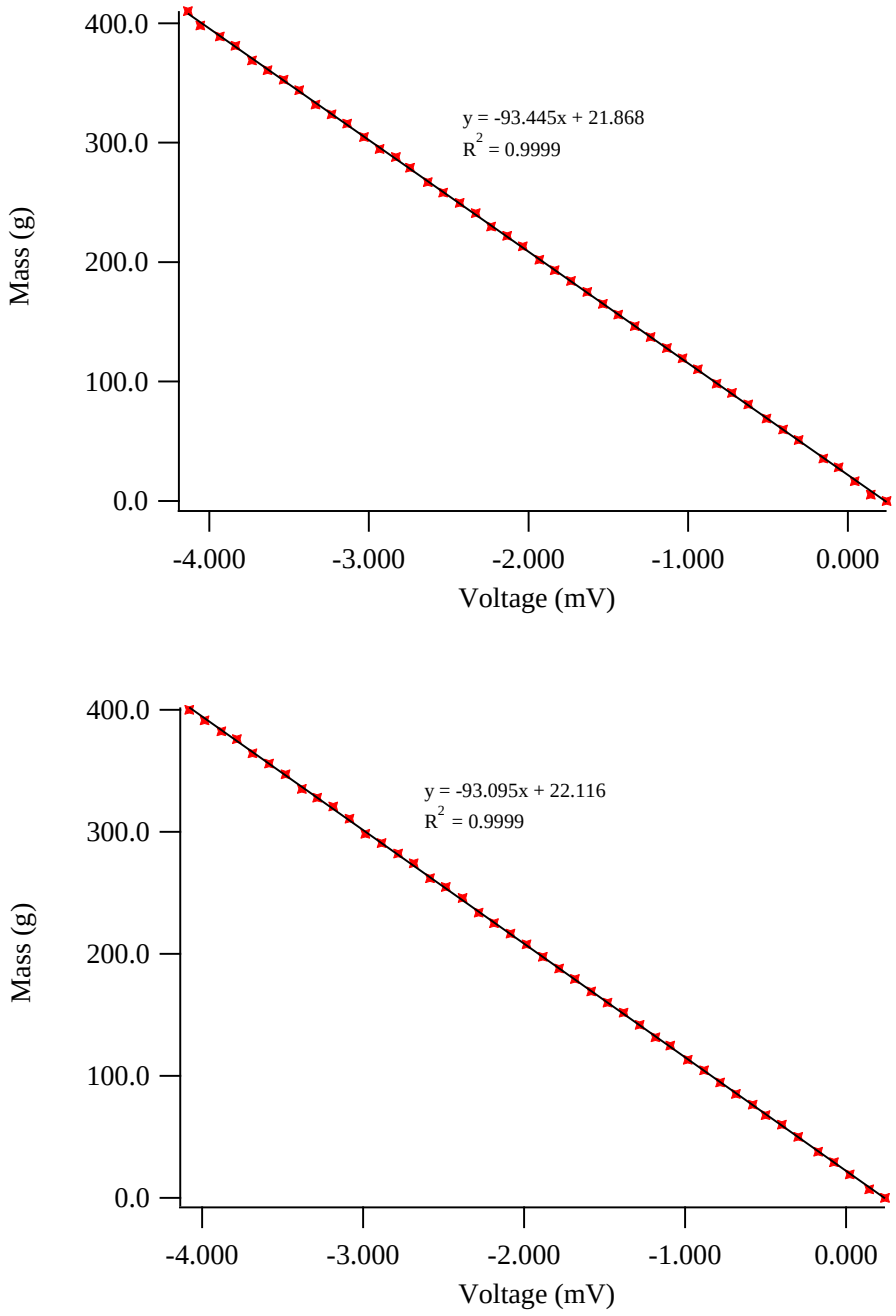

Figure S5. Calibration curves constructed for the second-generation force-measuring device. The slopes of these two plots agree with the linear fit presented in Figure 16 within error.

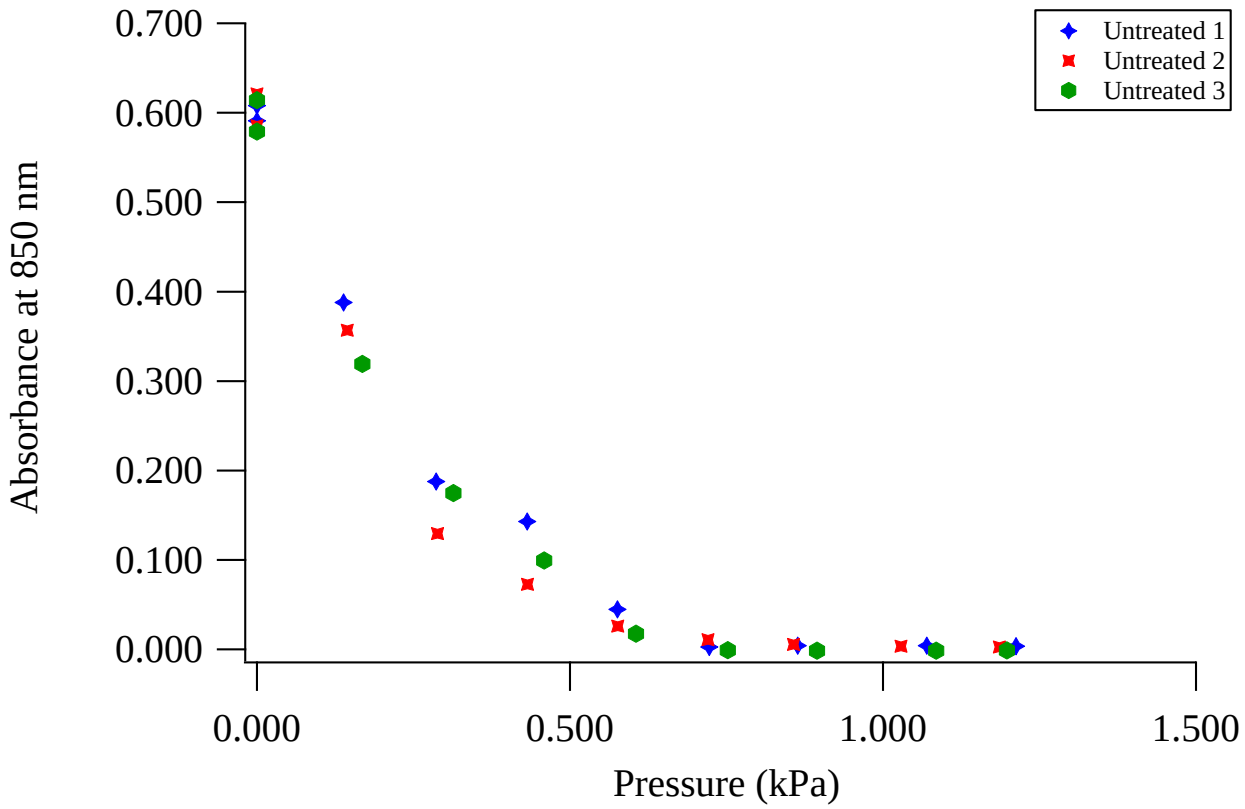

Figure S6. Absorbance-pressure curves generated for untreated Au-plated PMMA samples using the second generation force-measuring device. Sample 2 is presented in Figure 20. Au was deposited onto all samples using the same magnetron sputtering deposition parameters.

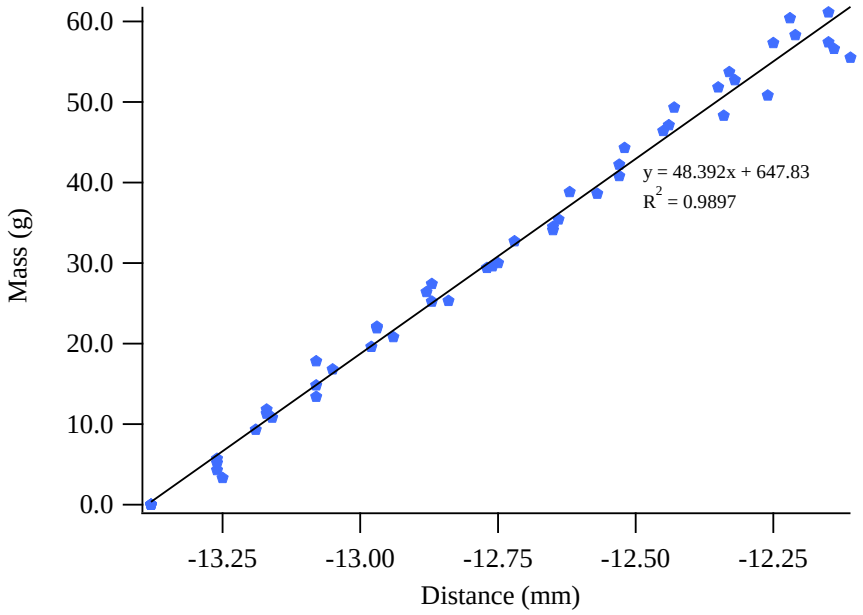

Figure S7. Calibration curve generated for the first generation force-measuring device prior to installing the modified spring system. Pressure 1 and 2 values for post-treated samples 2-6 and untreated samples 1-3 were calculated using this linear fit. The x-axis values represent the screw length caliper reading and are designated as negative to indicate an increasing change in distance from the initial caliper reading.

Appendix: Electron-beam Evaporation: Gold Deposition

Last Edited: 3/5/2014

1. Start up the computer.
2. Click on the green START icon located in the bottom left corner of your desktop, and proceed to click on the MB_EVAP icon.
3. A pop-up screen should appear. Click on "RUN." Note: you don't need a password, so just click "Ok" whenever you're asked to provide one.
4. You should now have three main windows open: a window in the bottom left-hand corner named SQS-242, a System Parameters window in the upper left-hand corner, and an MBraun Vacuum System Controller window that takes up the entire right side of the screen.
5. In the Vacuum System Controller window, there are two buttons at the bottom of the screen, "Auto" and "Manual" Click on the "Manual" setting.
6. Turn on the nitrogen source. On the side wall to the left of the monitor, there is a column of three levers with red handles, each of which should be pulled down parallel to the wall. Flip the top-most and bottom-most levers (not the middle one!!!), making sure the handles are perpendicular to the wall.
7. Go to the Vacuum System Controller window, and proceed to click on the "vacuum map" tab. Turn on the mechanical pump and press "Refill." Fill the chamber until the pressure reaches 1000 mbar (look at the Chamber Gauge for this information).

8. Once the pressure reached 1000 mbar, you can open the door to chamber. DO NOT OPEN THE CHAMBER IF THE INTERNAL PRESSURE IS LOWER THAN 1000 MBAR!!!
9. When opening the chamber, align the flat edge of the handle with the door. Vacuum out the chamber to remove any loose debris.
10. Place your samples on the purple rotary holder.
11. Screw rotary holder into the top of the chamber, with the purple side of the holder facing upward. Make sure to insert the two washers between the holder and the screw. Turning the screw counterclockwise tightens the screw; a clockwise turn loosens the screw.
12. Check rotary holder to make sure it is spinning properly. Go to the "evaporator functions" tab in the Vacuum System Controller window. Click on "Evaporator Rotary Holder." The rotary holder should be spinning when this button is green.
13. Check the substrate shutter to make sure it can open and close properly. Go to the "evaporator functions" tab and click on "Evaporator Substrate Shutter." This button should be red when the shutter is closed and green when the shutter is open.
14. Close the chamber door. Go back to the "vacuum map" tab and click on "Evacuate." You are now evacuating the chamber using the mechanical pump. Wait until the pressure reaches $1x10^{-1}$ mbar.
15. While you're waiting, record the following parameters: deposition rate (A/s), thickness deposited (A), rp (pressure after using mechanical pump), and cp (pressure after using the cryo pump). Include your initials and the date.

16. When the internal pressure reaches $1x10^{-1}$ mbar, turn off the mechanical pump (click "Evacuate" and turn on the cryo pump (click "Hi Vac Valve"). Wait until the pressure inside the chamber is 5×10^{-5} mbar.
17. While you're waiting, go to the SQS-242 window. Click [Edit => Process]. The process should be set to gold sputtering (goldsp). Makes sure the deposition rate is correctly set, typically at 1 A/s. [Set Pt]. Also, make sure the desired thickness of the Au thin film is set, typically either at 0.060 kA or 1.000 kA [Final Thick].
18. When the internal pressure reaches $5x10^{-5}$ mbar, focus your attention on the black circuit box located beneath the monitor. Flip the Main Power switch located in the bottom left-hand corner of the circuit box.
19. Wait 2-3 minutes.
20. Press the ON button located in the top right-hand corner of the circuit box under "Voltage/Emission."
21. If the entire power supply cuts off, you have open the cabinet located next to the circuit box and flip the switch. Wait at least 10 minutes before attempting to turn on the power again.
22. Go to the SQS-242 window and click on "Start Process."
23. Wait for 3 minutes and 30 seconds while the Ramp 1, Soak 1, and Ramp 2 phases proceed.
24. Go the "evaporator functions" tab. When the "Shtr Delay" phase is reached, be ready to open the substrate shutter by clicking on "Evaporator Substrate Shutter." The Shtr Delay phase typically lasts about 40 seconds.
25. Keep the shutter open during the deposit phase.

26. Record the temperature of the cryo pump during deposition.
27. Close the substrate shutter after depositing the desired amount of Au onto your samples. The area that says “Thick[kA]” tells you the amount of gold in kA that has been deposited.
28. Press the OFF button, located right next to the ON button, and wait for 2 minutes.
29. Turn of the main power supply.
30. Turn off cryo pump (Press “Hi Vac Valve” under the “vacuum map” tab) Press “Refill” and fill the chamber until the pressure reaches 1000 mbar.
31. Open the substrate shutter (“Evaporator Substrate Shutter”) and stop the rotary holder (“Evaporator Rotary Holder”).
32. You can now open the chamber and remove your samples.
33. Close the chamber door and evacuate the chamber until the pressure reaches either 10 or 20 mbar.
34. Press “Auto” in the Vacuum System Controller Window. Turn off the mechanical pump (but not the cryo pump!)
35. Turn the nitrogen off.
36. Exit out of the program.
37. Shut the computer off.

Troubleshooting:

1. If the power cuts off when you press the ON button, check for flipped switch and wait for 10 minutes.

2. If it takes 30 minutes or more for the scroll pump to evacuate the chamber to $1X10^{-1}$ mbar, something needs to be replaced. Find Harry Hu for assistance.
3. In the SQS-242 window, click “view” and then “sensor” reading. If the lifetime is 20% or less, the supply of gold is too low.
4. Make sure the door of the cabinet with the switches is latched tightly.
5. Vacuum up loose debris from vacuum chamber.
6. Clean & use nitrogen air compressor.

Simplified Instructions for Operating the Edwards Auto 500 Magnetron Sputtering System (a.k.a. Magnetron Sputtering for Dummies)

Last Edited: 10/12/2015

Important Terminology

Vacuum Chamber and Turbo Pump

Magnetron Control Center

DC Power Supply

Gas Flow Control Panel

Big Black Control Panel

Edwards AUTO 500 Magnetron Sputtering System Control Panel

Vacuum System Control Panel

Turning on the Instrument

1. ***Turn the water on***. The water flow meter is located behind the Magnetron, next to an electrical outlet and a vent. Pull the yellow handle up so that the float in the water flow meter is at 0.5 to 0.6 GPM. It may be noisy, but don't panic!! This is typical.

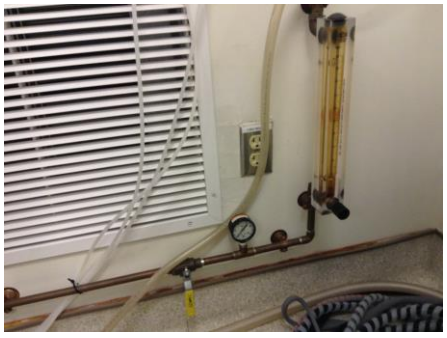

2. Press the green “On” button, which is located on the *Edwards AUTO 500 Magnetron Sputtering System Control Panel*. At this point, the green “Vacuum System” and “Control Cabinet” indicators should light up.

3. Rotate the black switch from “0” to “1.” This switch is located at the top of the *Big Black Control Panel*.

4. Go to the *Vacuum System Control Panel*. First press the “Reset” button, then press the “Start” button.
5. Take the black key, insert it into the black keyhole located underneath the vacuum chamber, and turn the key a ¼ turn counterclockwise.

6. Once you’ve opened the door, you should see a blue “Start/Stop” button. If the green light does not turn on within 5-10 minutes, press the button.

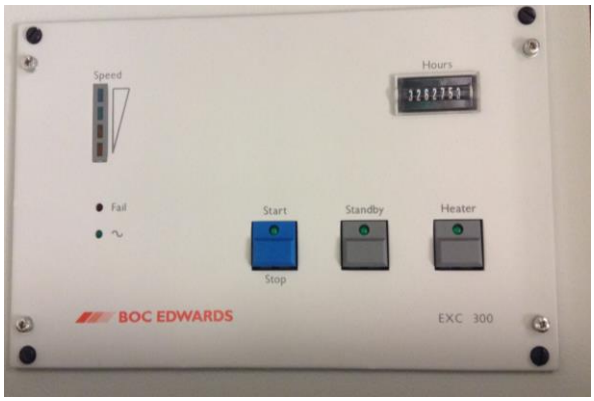

7. The turbo pump should start spinning up. A series of four lights is present on the same control box as the "Start/Stop" button. As soon as the pump has spun all the way up, the two right hand lights should appear orange and the two left hand lights should appear green. You can then proceed to fill the vacuum chamber.

Filling the Vacuum Chamber

1. You will see three red valves located behind the Magnetron. To turn on the nitrogen gas supply, flip the bottom two valves so that they are pointing outward from the wall. The top valve opens the N_2 supply to the e-beam deposition system, so you **DO NOT** need to flip this valve.

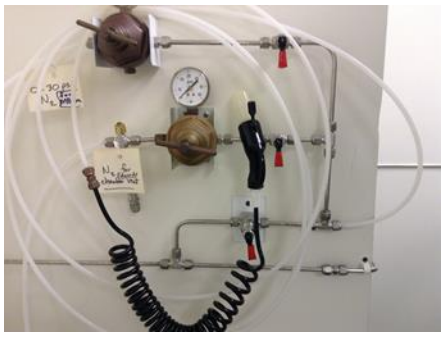

2. To fill the chamber with N_2, press the "Vent" button, which is located on the *Vacuum System Control Panel*. The pressure inside the chamber should reach 760 Torr (as shown in the image below).

3. To open the chamber, pull up on the black handle that's attached to the right side of the chamber door. Even though the chamber pressure gauge may read 760 Torr, if you cannot open the door, then the pressure inside the chamber has not reached atmospheric pressure. **Wait until you can push up the handle and open the door with little effort**.

Placing Samples in the Chamber

1. Unscrew the purple rotary sample holder from the chamber ceiling. Use the metal wrench with the red rubber handle. If the bolt/screw that holds the sample holder in place is not visible or accessible, see Step 4 to learn how to rotate the holder to access the bolt.

2. Place the plate (sample holder) on clean Berkshire© wipes on the table top. Load samples into the windows from the backside of the plate. Make sure that the side onto which you're trying to deposit metal is facing downward.

3. Slip the plate onto the shaft in the top of the chamber. When the screw on the holder is aligned with the groove in the shaft, use the wrench with a red handle to tighten the screw. The screw keeps the plate from slipping back off the shaft, so make sure it is snug. However, do NOT overtighten the screw.

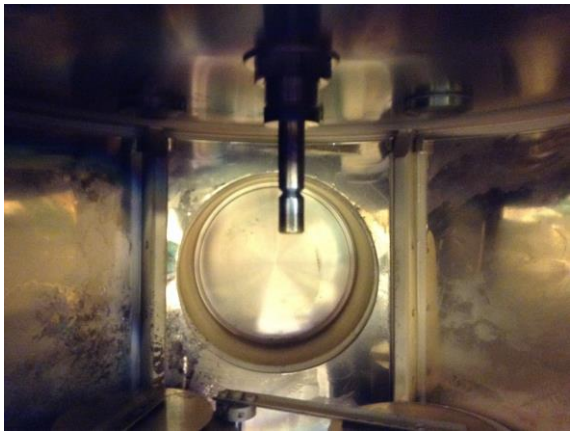

4. Go to the *Big Black Control Panel*. To start rotating the holder, press both the start button and the button located to the left of this button. Both of these buttons should be pressed **IN**. This should make the plate rotate. The green light located next to these buttons should come on.

5. Make sure the shutter over the target you plan to use is working. Shutter 1 is over the front left target, Shutter 2 is over the rear left target, and Shutter 3 is over the rear right target. The *Big Black Control Panel* contains two "Source Shutter" panels. If you need to use Target 1 or Target 2, go to the left panel and press either the SS 1 or SS 2 button, respectively. If you need to use Target 3, go to the right panel and press the SS 1 button. When the button is pushed **IN**, the shutter is open. When the button is pushed **OUT**, the shutter is closed.

6. If you have dropped anything in the chamber, you **MUST** find it and remove it before proceeding. Seek assistance if necessary. Carefully look for metal flakes and metal peelings anywhere in the chamber and remove loose metal with the vacuum cleaner at the sticky side of adhesive tape.
7. Once you're sure that the shutter is working and the sample holder is rotating, close the chamber door.

Evacuating the Chamber

1. Go to the *Vacuum System Control Panel*. Press the "Cycle" button, which is located directly next to the "Vent" button. At this point, you need to wait until the chamber pressure inside the chamber reaches 9.0 e^{-5} Torr. This process will take about 10-15 minutes. About 2-3 minutes in, you'll hear a small "pop." Don't be alarmed! This just means the pumping is switching from the mechanical pump to the Turbo pump. While you're waiting, you can set the timer to the amount of time for which you would like to carry out the deposition.
2. Once the pressure reaches 9.0 e^{-5} Torr, proceed to complete this next series of steps, which can be completed in any order.
    a. Turn the yellow handle of the water flow meter up so that the water level is all the way up above 2.0. The green "Water Cooling" light should come on.
    b. Go to the right hand blue-green gas tank located behind the E-beam. The white label should indicate that the tank contains compressed argon. Turn the knob at the top of this tank a few rotations counterclockwise. The other tank contains Ar/O_2, which is needed only when depositing metal oxides.

c. Go to the *Gas Flow Control Panel*. Flip the "Power" switch up.

d. Go to the "1" switch. This switch has three positions: down, level, and up. Pull this switch up so that it is in the "level" position.

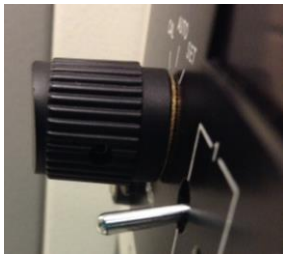

Down

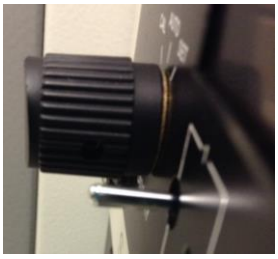

Level

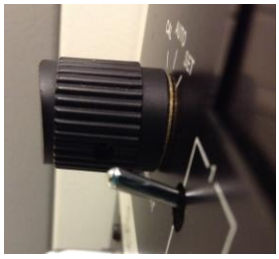

Up

3. Go to the *DC Power Supply*. Press in the "Power" button so that the red light turns on.

4. At this point, check the chamber pressure. Once the pressure is at or below 7.0 e^{-5} Torr, record both this pressure and the back pressure. You view the back pressure reading by pressing the down arrow button. You can then return to viewing the chamber pressure by pressing the up arrow button.

5. Press the “Seal” and then the “Process” button. If you do this properly, the green “Sputtering Enabled” light will come on. At this point, all four system interlocks present on the *Edwards AUTO 500 Magnetron Sputtering System Control Panel* should be lit up.

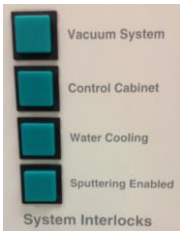

6. Shortly after the “Sputtering Enabled” light turns on, the green “Gas Control Enabled” light will come on. This indicator is located next to the *Gas Flow Control Panel*. Once this occurs, you can press the “Gas 1 Enabled” button.

Metal Deposition

1. Make sure you know which DC Power Supply you need to use. The upper supply provides power to Target 3. The lower supply provides power to Target 1 or Target 2. The “RF & DC Power Selector Switch” in the *Big Black Control Panel* must be set to Source 2 DC in order to use Target 2.
2. Go to the “Right Display” area on the *DC Power Supply* and press the “SETPT” button. Turn the black “Level” knob to adjust the power. Turning the knob clockwise increases the power. Set the power to 30W.

3. Go to the "Output" square present on the *DC Power Supply* and press the "On" button. The four indicators shown here should light up.

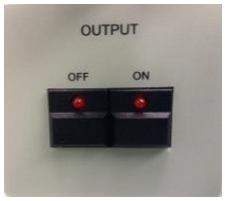

4. To generate the plasma, go to the *Gas Flow Control Panel* and turn the "1" switch to the "up" position. If the red "PLASMA" indicator does not light up in Step 3, then implementing Step 4 will cause this to happen.
5. Turn the "1" switch back down to the "level" position.
6. Go back to the *DC Power Supply* and turn the "Level" knob until you reach the desired wattage, but no more than 300W. With the "SETPT" button, the set wattage will read two watts higher than the actual power. You can press the "ACTUAL" button to view the actual wattage. The "SETPT" button can also be used to view the current and the voltage. Simply press the button until you reach the desired parameter, which is indicated to the right of the digital reading.
7. Start the timer and press the shutter button **IN** at exactly the same time. This opens the shutter and starts depositing metal.

8. While you're waiting for the timer to go off, record the chamber pressure, the back pressure, and the Argon gas flow, which is in units of sccm and can be read off the *Gas Flow Control Panel*.

9. Press the shutter button back **OUT** as soon as the timer goes off. This closes the shutter and stops the metal deposition.
10. Go to the *DC Power Supply* and turn the "Level" knob counterclockwise until the wattage is back down at 30W. You can then push the "off" button located in the Output box and the power button.
11. Press the "Gas 1 Enabled" button so this light goes off.
12. Go to the *Gas Flow Control Panel*. Push the "1" switch to the "down" position, and flip the power switch so that the lever is down. Go to the Ar gas tank and turn the knob clockwise until you can no longer turn it.
13. Go to the water flow meter and push down the handle so that the float in the water flow meter is at 0.5 - 0.6 GPM.

Removing Samples from the Vacuum Chamber

1. Go to the *Vacuum System Control Panel*. First press the "Seal" button, the press the "Vent" button. Wait until the chamber pressure reaches 760 Torr. Once again, the chamber door will automatically unlock. DO NOT try to force the door open.

2. Go to the *Big Black Control Panel* and press the rotary holder buttons **OUT**. Time this so that the rotary holder stops spinning with the screw facing towards you. Remove the rotary holder from the vacuum chamber.
3. Once you have taken your samples out of the rotary holder, screw the holder back into the chamber and close the door. Repeat Step 1 from *Evacuating the Chamber*. While you're waiting for the pressure to reach 9.0 e^{-5} Torr, turn off the N_2 gas by flipping the two red valves down.
4. Once the chamber pressure reaches 9.0 e^{-5} Torr, go to the *Vacuum System Control Panel* and press the "Seal" button. At this point, you do not have to shut the instrument off if you plan on using it in the imminent future.

Shutting the Sputtering System Off

1. If nobody is planning on using the Magnetron for a while (at least for a weekend), then you need to completely shut the instrument off. First, go to the *Vacuum System Control Panel* and press the "Stop" button after pressing the "Seal" button. At this point, the turbo pump will power down. This can take up to an hour, so find something else to do while you're waiting!
2. You can proceed to the next step once all four of the lights present on the turbo pump control box have gone off. Go to the *Big Black Control Panel* and turn the black switch from "1" back to "0."
3. Press the red "Off" button, located under the green "On" button on the *Edwards AUTO 500 Magnetron Sputtering System Control Panel*.
4. Make sure the door located underneath the vacuum chamber is locked.

5. Go to the water valve and push down the yellow handle until you've turned the water supply off. Do **NOT** cut off the water supply as long as the turbo pump is running!!!!!!

A Few Notes about Using the Timer

1. There are two yellow switches present on the right side of this timer. The bottom switch controls which timer is being used (T1, T2, or T3). The top switch has two settings: "Lock" and "Set." Use "Set" when setting the timer. Use "Lock" once you've set the desired time and are ready to run the timer.
2. You need to use considerable force when pressing the "Clear," "Memory," or "Start/Stop" buttons.

IMPORTANT NOTES

Choosing a Metal Target

- As you've probably noticed, there are two *DC Power Supply* panels. The top panel controls Targets 1 and 2. On the *Big Black Control Panel*, there is a knob that controls which target is in use (see image below). Use either "Source 1 DC" or "Source 2 DC." The bottom panel controls Target 3.

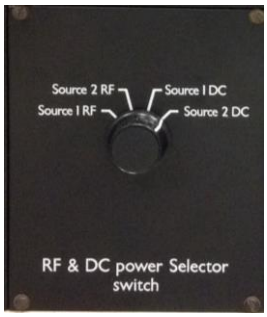

- As of 5/28/15, Target 1 contains manganese, Target 2 contains chrome, and Target 3 contains gold. This is subject to change at any time. Check the Magnetron Sputtering System lab notebook to see the most updated schematic of each target.

Troubleshooting

- The most important step of the sputtering process is ensuring that the float in the water flow meter is ALL THE WAY ABOVE 2.0 DURING PLASMA GENERATION AND METAL DEPOSITION!!!! Water is needed to cool the pump and the target guns, so overheating is very bad.
- Because the water used to cool the system comes from a public source, fluctuations of the water level can result from the use of a sink or the flush of a toilet. Regularly monitor the water level during both the plasma generation and metal deposition steps.
- Once the chamber pressure has reached $7.0e^{-5}$ Torr or lower, you are supposed to press the "Seal" and then the "Process" button. Sometimes, if you wait too long to press the "Seal" button, the "Sputtering Enabled" light will not come on. If this light does not come on after 5 minutes, press the "Seal" button and then the "Cycle" button, then wait until the pressure reaches $7.0e^{-5}$ Torr again.

Suggested Recipes for Gold Sputtering

- 75W for 90s – approximately 300 Å
- 150W for 7 min. – approximately 1300 Å

Vacuuming the Chamber

- If you start seeing metal flakes appear at the bottom of the chamber, vacuum out the chamber floor. Especially make an effort to remove flakes from the ¼ inch disk that is the valve of the Turbo pump. Flakes can get sucked into the pump, and this needs to be avoided at all costs.
- If flaking occurs on the walls, use scotch tape to rip off the metal. Store pieces of tape in the appropriate Zip Lock bag, which is located in the beige supply cabinet.

Format for Recording Parameters in Lab Notebook

Date Initials Chamber Pressure before Deposition Back Pressure before Deposition

Power during Deposition Ar Gas Flow

Chamber Pressure during Deposition Back Pressure during Deposition

Time of Deposition Rotation On

Example:

5/28/15 KK $P_{ch} = 7.0e^{-5}$ $P_{back} = 4.2e^{-2}$

75W Ar flow = 4.81

$P_{ch} = 2.3e^{-3}$ $P_{back} = 6.0e^{-2}$

90s Dep. Rot. On.